Preface to the Book Series

To train young people to grind lenses… . I cannot see there would be much use…because most students go there to make money out of science or to get a reputation in the learned world. But in lens-grinding and discovering things hidden from our sight, these count for nought.

—Antonie van Leeuwenhoek

Letter to Gottfried Leibniz on 28 September 1715 in response to Leibniz' request that he should open a school to train young people in microscopy

You can observe a lot just by watching.

—Yogi Berra

ONE OF THE CENTRAL THEMES OF BIOLOGY IS the constant change and transformation of most biological systems. In fact, this dynamic aspect of biology is one of its most fascinating characteristics, and it draws generation after generation of students absorbed in understanding how an organism develops, how a cell functions, or how the brain works. This series of manuals covers imaging techniques in the life sciences—techniques that try to capture these dynamics. The application of optical and other visualization techniques to study living organisms constitutes a direct methodology to follow the form and the function of cells and tissues by generating two- or three-dimensional images of them and to document their dynamic nature over time. Although it seems natural to use light to study cells or tissues, and microscopists have been doing this with fixed preparations since van Leeuwenhoek's time, the imaging of living preparations has only recently become standard practice. It is not an overstatement to say that imaging technologies have revolutionized research in many areas of biology and medicine. In addition to advances in microscopy, such as differential interference contrast or the early introduction of video technology and digital cameras, the development of methods to culture cells, to keep tissue slices alive, and to maintain living preparations, even awake and behaving, on microscopes has opened new territories to biologists. The synthesis of novel fluorescent tracers, indicator dyes, and nanocrystals and the explosive development of fluorescent protein engineering, optogenetical constructs, and other optical actuators like caged compounds have made possible studies characterizing and manipulating the form and function of cells, tissues, and circuits with unprecedented detail, from the single-molecule level to that of an entire organism. A similar revolution has occurred on the optical design of microscopes. Originally, confocal microscopy became the state-of-the-art imaging approach because of its superb spatial resolution and three-dimensional sectioning capabilities; later, the development of two-photon excitation enabled fluorescence imaging of small structures in the midst of highly scattered living media, such as whole-animal preparations, with increased optical penetration and reduced photodamage. Other

nonlinear optical techniques, such as second-harmonic generation and coherent anti-Stokes Raman scattering (CARS), now follow and appear well suited for measurements of voltage and biochemical events at interfaces such as plasma membranes. Finally, an entire generation of novel "superresolution" techniques, such as stimulated emission depletion (STED), photoactivated localization microscopy (PALM), and stochastic optical reconstruction microscopy (STORM), has arisen. These techniques have broken the diffraction limit barrier and have enabled the direct visualization of the dynamics of submicroscopic particles and individual molecules. On the other side of the scale, light-sheet illumination techniques allow the investigator to capture the development of an entire organism, one cell at a time. Finally, in the field of medical imaging, magnetic resonance scanning techniques have provided detailed images of the structure of the living human body and the activity of the brain.

This series of manuals originated in the Cold Spring Harbor Laboratory course on Imaging Structure and Function of the Nervous System, taught continuously since 1991. Since its inception, the course quickly became a "watering hole" for the imaging community and especially for neuroscientists and cellular and developmental neurobiologists, who are traditionally always open to microscopy approaches. The original manual, published in 2000, sprang from the course and focused solely on neuroscience, and its good reception, together with rapid advances in imaging techniques, led to a second edition of the manual in 2005. At the same time, the increased blurring between neuroscience and developmental biology made it necessary to encompass both disciplines, so the original structure of the manual was revised, and many new chapters were added. But even this second edition felt quickly dated in this exploding field. More and more techniques have been developed, requiring another update of the manual, too unwieldy now for a single volume. This is the reasoning behind this new series of manuals, which feature new editors and a significant number of new methods. The material has been split into several volumes, thus allowing a greater depth of coverage. The first book, *Imaging: A Laboratory Manual*, is a background text focused on general microscopy techniques and with some basic theoretical principles, covering techniques that are widely applicable in many fields of biology and also some specialized techniques that have the potential to greatly expand the future horizon of this field. A second manual, *Imaging in Neuroscience: A Laboratory Manual*, keeps the original focus on nervous system imaging from the Cold Spring Harbor Imaging course. A third volume, *Imaging in Developmental Biology: A Laboratory Manual*, now solely deals with developmental biology, covering imaging modalities particularly suited to follow developmental events. There are plans to expand the series into ultrastructural techniques and medical-style imaging, such as functional magnetic resonance imaging (fMRI) or positron emission tomography (PET), so more volumes will hopefully follow these initial three, which cover mostly optical-based approaches.

Like its predecessors, these manuals are not microscopy textbooks. Although the basics are covered, I refer readers interested in a comprehensive treatment of light microscopy to many of the excellent texts published in the last decades. The targeted audience of this series includes students and researchers interested in imaging in neuroscience or developmental or cell biology. Like other CSHL manuals, the aim has been to publish manuals that investigators can have and consult at their setup or bench. Thus, the general philosophy has been to keep the theory to the fundamentals and concentrate instead on passing along the little tidbits of technical knowledge that make a particular technique or an experiment work and that are normally left out of the methods sections of scientific articles.

This series of manuals has only been possible because of the work and effort of many people. First, I thank Sue Hockfield, Terri Grodzicker, Bruce Stillman, and Jim Watson, who conceived and supported the Imaging course over the years and planted the seed blossoming now in these manuals and, more importantly, in the science that has spun out of this field. In addition, the staff at CSHL Press has been exceptional in all respects, with special gratitude to John Inglis, responsible for an excellent team with broad vision, and David Crotty, who generated the ideas and enthusiasm behind this new series. Also, Inez Sialiano, Mary Cozza, Michael Zierler, Kaaren Janssen, Catriona

Simpson, Virginia Peschke, Judy Cuddihy, Martin Winer, Kevin Griffin, Kathleen Bubbeo, Lauren Heller, Susan Schaeffer, Jan Argentine, and Denise Weiss worked very hard, providing fuel to the fire to keep these books moving, and edited them with speed, precision, and intelligence. More than anyone, they are the people responsible for their timely publication. Finally, I honor the authors of the chapters in these books, many of them themselves past instructors of the CSH Imaging course and of similar imaging courses at institutions throughout the world. Teaching these courses is a selfless effort that benefits the field as a whole, and these manuals, reflecting the volunteer efforts of hundreds of researchers, who not only have taken the time to write down their technical knowledge but have agreed to generously share it with the rest of the world, are a beautiful example of such community cooperation. As Leibniz foresaw, "lens grinding" is a profession that is indeed meaningful and needs the training of young people.

— RAFAEL YUSTE

Index

A

AceBatch software, 803, 809, 811
AceTree software, 803, 805–809, 806f, 810–811, 812
Acetylcholine receptors (AChRs), 437, 439
ACSF solution (1x) (recipe), 354
ACSF stock solution A (recipe), 354
ACSF stock solution B (recipe), 354
Actin promoter, 32
Action potential firing, 491–492, 497
Adeno-associated virus (AAV)
  Cre-dependent adeno-associated virus preparation and delivery (protocol), 209–213
Adobe Image Ready CS, 255
Afferent neurons of lateral-line system, labeling, 283–284, 283f
AFP-GFP transgenic line, 300
Afp promoter, 103, 104
Agar mounts
  preparation for observation of *Caenorhabditis elegans* embryos (protocol), 231–234
    agar pad preparation, 233f
    discussion, 234
    experimental method, 232–233
    imaging setup, 231
    isolation of embryos and preparation for mounting, 232f
    materials, 231
    troubleshooting, 233–234
  for zebrafish embryos, 274
Agarose
  albumin-agarose (recipe), 604
  embedding mouse embryo in, 748, 749f
  embryo embedding agarose (recipe), 267
  low-melting-point agarose (recipe), 432
  as mounting media
    difficulties with, 274
    mouse retina, 422
    zebrafish embryos, 262
  recipe for 0.5% w/v, 763
Albumin-agarose (recipe), 604
Alexa 594 dye, 482, 483f, 484
Alexa Fluor 647-conjugated α-bungarotoxin, 437, 442
Alexa Fluor 488 dextran 3000, 147–148, 147f
α-actinin2, 206
Ames medium (recipe), 432
Amira software (Visage Imaging), 420, 795
Anesthesia
  fly, 38
  mouse, 516, 673
  zebrafish embryo, 59, 59f, 273, 274
Anesthetic medium (recipe), 384
Anterior visceral endoderm cells, movement of, 299–300
Antibody
  anti-GFP, 526, 527f
  imaging synapse formation and function in neuronal cell cultures by quantitative immunocytochemistry, 468–476
  staining of bicoid-GFP *Drosophila* embryos, 526, 527f
APC^{Cdh1} complex, 332
Apple juice agar (recipe), 43, 696
Arc lamp, 833–834
Arima software, 718–723, 721f–723f
Artificial cerebrospinal fluid (aCSF) (recipe), 432, 432t, 510
Artificial cerebrospinal fluid (aCSF) stock solutions, 354
Artificial seawater-HEPES (ASWH) (recipe), 727
Ascidian embryos, creating 3D digital replicas of, 711–728
Atlas
  anatomical, optical projection tomography (OPT) and, 743
  developmental, 7–8
    labeling anatomy, 794–795, 796f
    microscopic magnetic resonance imaging (μMRI), 793–797
    mouse, 794
    quail, 794, 795f
    visualizing developing anatomy from atlases, 796–797
  gene expression, 702–703
Atrial septal defects, 647
Atrioventricular septal defects, 647
attP sites, 33
Autofluorescence
  in *Drosophila* embryos, 25
  in *Drosophila* larvae, 26
Automated lineage in *Caenorhabditis elegans* embryos, 799–814
  automated lineage analysis and expression mapping (protocol), 801–813
    discussion, 813
    experimental method, 803–811
    automated lineage analysis, 804–805, 805f
    curating/editing lineage (advanced), 808–809
    curating/editing lineage (basic), 807–808
    export, 811
    imaging, 804
    reporter signal extraction, 809–810, 810f
    strain generation, 803
    viewing, 810–811
    viewing lineage in AceTree, 805–806, 806f
  imaging setup, 801–803, 802t
  materials, 803
  troubleshooting, 811–812
  overview, 799–800
Avian embryos. *See also* Chick embryos
  four-dimensional fluorescent imaging of quail development, 593–604
  live imaging, 85–99
  optical coherence tomography (OCT) imaging of beating heart, 647–655
Axiovision, 274
Axonal specification, 458, 458f
Axonal transport of vesicles, 461–462, 462f
Axon pathfinding, imaging, 373–386
  overview, 373–374
  in *Xenopus,* 373, 375–380, 384
    experimental method, 376–378
      imaging, 378, 379f
      preparing and mounting embryos, 376–378, 376f, 377f
    imaging setup, 375
    materials, 375
    troubleshooting, 376–378
  in zebrafish, 381–383, 384
    experimental method, 382
      imaging, 382, 383f
      preparing and mounting of embryos, 382
    imaging setup, 381
    materials, 381
    troubleshooting, 382
Axons
  labeling, 436–437
  simultaneous imaging of structural plasticity and calcium dynamics

Page references followed by f denote figures; page references followed by t denote tables.

Axons (*Continued*)
in developing, 479–489
overview, 479–480
protocol, 481–489
bolus labeling of neuronal structures, 483, 483f
confocal imaging, 485
discussion, 487
electrode preparation, 483
electroporation of individual cells, 484
experimental method, 482–486, 483f, 486f
hippocampal slice preparation, 482–483
image analysis, 484f, 485–486, 486f
imaging setup, 481
materials, 482
recipes, 488–489
troubleshooting, 486
in vivo imaging in developing cortex in mice, 513–522
overview, 513–514
protocol, 515–521
application example, 520, 520f, 521f
discussion, 520–521
experimental method, 516–518
imaging setup, 515
materials, 515–516
troubleshooting, 518–519
in vivo time-lapse imaging of neuronal development in *Xenopus,* 387–404
Azam-Green, in Fucci probe, 332, 332f

B

Background removal, 691–693, 692f
Bacterial artificial chromosome (BAC)
Gene Expression Nervous System Atlas (GENSAT) project and, 608
transgene expression in zebrafish, 408–409, 408f
transgenic approach to genetic labeling of neurons in mouse brain, 200–201, 201f, 206
Ballistic labeling of developing retinal neurons, 177–190
applications, 187, 188f
depth of labeling, 187
gene gun
applications, 187
depth of labeling, 187
protocol for use of, 185–186
tissue damage, 187
image acquisition, 189
intensity of labeling, 187–189
overview, 177
protocols
coating gold particles with DNA (biolistics), 183–184
coating particles with carbocyanine dyes, 178–180, 179f
coating particles with dextran-conjugated fluorescent dyes, 181–182
shooting DNA, dyes, or indicators into tissue slices using the gene gun, 185–186
troubleshooting, 187
tissue damage, 187
BAPTA, 367
BAPTA-AM, 366
BAPTI (birthdating analysis by photoconverted fluorescent protein tracing in vivo)
overview, 245–246
protocol, 248–250
schematic, 246f
uses of, 251
BAPTISM (birthdating analysis by photoconverted fluorescent protein tracing in vivo combined with subpopulation markers)
overview, 246
protocol, 248–250
schematic, 247f
use of multiple markers, 251
uses of, 251
Bassoon, 406
Bathing saline solution (recipe), 476
BB/BA solution, 733, 746, 750
Beam splitter, dichroic, 829f, 830
Benzyl benzoate (BB)/benzyl alcohol (BA) for clearing of *Xenopus embryos,* 733
Berkeley *Drosophila* Transcription Network Project (BDTNP), 699
β-actin promoter, 454
Bicoid (*Drosophila*), 29
Bicoid morphogen gradient, quantifying experimental procedures
antibody staining, linearity of, 526, 527f
calculating absolute bicoid concentration, 528–529, 528f, 529f
fly strain generation, 525–526
imaging of live embryos, 526, 528
microscopy apparatus, 524–525, 524–530, 525f
quantification of errors, 530
reproducibility across embryos, measuring, 529–530
overview, 523–524, 530–531
Binary expression systems, genetic labeling of neurons in mouse brain and
Cre/*loxP* system, 203f, 204
direct labeling compared, 208
gene targeting and, 202–203, 202f, 203f
viruses as reporters in, 205–206, 205f
Biolistic DNA transfection, of developing retinal neurons, 183–184, 187
Biosensors, use of in *Drosophila,* 29, 30t
Birthdating in zebrafish, 245–252
overview, 245–247
BAPTI (birthdating analysis by photoconverted fluorescent protein tracing in vivo), 245–246, 246f
BAPTISM (birthdating analysis by photoconverted fluorescent protein tracing in vivo combined with subpopulation markers), 246, 247f
BrdU labeling compared, 246
protocol, 248–250
BAPTI procedure, 249–250
BAPTISM procedure, 250
example application, 250
experimental method, 248–250
imaging setup, 248
materials, 248
photoconversion, 249
recipes, 251
Birth defects, 647–648
Blastoderm, three-dimensional morphology and gene expression mapping in *Drosophila,* 699–710
pipeline, 703–707
conversion of images to point clouds, 704–706, 705f
PointCloudXplore visualization tool, 706–707, 708f
registration of point clouds into a virtual embryo, 706, 707f
staining, mounting, and imaging, 703–704
temporal staging, 704
strategy, 700–703
high-throughput imaging and analysis, 702–703
pattern dynamics, 701–702
Blastomeres
in *Caenorhabditis elegans* embryos, 229–244
acquisition of 4D DIC microscopic data to determine cell contacts (protocol), 235–238
discussion, 238
experimental method, 236–237
imaging setup, 235
materials, 236
troubleshooting, 237–238
agar mount preparation for observation of (protocol), 231–234
agar pad preparation, 233f
discussion, 234
experimental method, 232–233
imaging setup, 231
isolation of embryos and preparation for mounting, 232f
materials, 231
troubleshooting, 233–234
analysis of 4D DIC microscopic data to determine cell contacts (protocol), 239–240
discussion, 240
experimental method, 239–240
imaging setup, 239
materials, 239
troubleshooting, 240
laser killing of blastomeres (protocol), 241–242
discussion, 242
experimental method, 241–242
imaging setup, 241
materials, 241
troubleshooting, 242
injection of cleavage-stage zebrafish embryos and imaging of labeled cells (protocol), 571–578
discussion, 577
experimental method, 572–576
imaging, 575–576
imaging setup, 571
labeling embryos, 572–573
materials, 571–572
mounting, 574–575
recipes, 578
troubleshooting, 576–577

Bleach, for removal of chorion membrane, 526
Bleaching, of *Xenopus embryos,* 733
Blood cells, ε-globin-GFP expressing, 663, 664f
Blood flow, Doppler imaging of, 666–667
Bloomington Stock Center, 33
Bolus labeling of neuronal network, 483, 483f
Boyd buffer (recipe), 20
Brainbow, 3
  genetic labeling of neurons in mouse brain, 207
  imaging in zebrafish, 191–198
    example application, 197
    overview, 191–192, 192f
    protocol, 193–196
      Cre recombinase introduction, 193–194
      materials, 193
      plasmid selection, 194
      recipes, 197
      troubleshooting, 195–196
    transgenic construct, 192f
Brenner, Sydney, 11
BREReA software, 689

C

Cadherins, 406
Caenorhabditis elegans
  automated lineage and expression profiling in, 799–814
    automated lineage analysis and expression mapping (protocol), 801–813
      discussion, 813
      experimental method, 803–811
      imaging setup, 801–803, 802t
      materials, 803
      troubleshooting, 811–812
    overview, 799–800
  cell contact and cell polarity in embryos, 229–244
    overview, 229–230
    protocols
      acquisition of 4D DIC microscopic data to determine cell contacts, 235–238
      agar mount preparation, 231–234
      analysis of 4D DIC microscopic data to determine cell contacts, 239–240
      laser killing of blastomeres, 241–242
      recipes, 243
  embryogenesis overview, 12
  live imaging of embryogenesis, 11–21
    differential interference microscopy, 12, 12f
    fluorescence microscopy, 12–14
      phototoxicity, 13
      signal loss issues, 13
      temperature control, 13–14
    mounting embryos (protocol), 15–19
    overview, 11
    recipes, 20
  as model system, 11
Caged fluorescein, 277
CAGG promoter, 204
CAG-KikGR transgenic line, 301
CAG-TAG transgenic line, 300f, 301
Calcium blocker cocktail (recipe), 369
Calcium-free saline (recipe), 369
Calcium imaging
  calcium dynamics in developing dendrites and axons, 479–489
    overview, 479–480
    protocol, 481–489
      bolus labeling of neuronal structures, 483, 483f
      confocal imaging, 485
      discussion, 487
      electrode preparation, 483
      electroporation of individual cells, 484
      experimental method, 482–486, 483f, 486f
      hippocampal slice preparation, 482–483
      image analysis, 484f, 485–486, 486f
      imaging setup, 481
      materials, 482
      recipes, 488–489
      troubleshooting, 486
  simultaneous patch-clamping and calcium imaging in developing dendrites, 491–498
    overview, 491–492
    protocol, 493–497
      data acquisition, 494–495, 494f
      discussion, 497
      experimental method, 494–495
      imaging setup, 493
      materials, 493–494
      patch procedure, 494, 494f
      recipes, 497
      troubleshooting, 495–496
Calcium indicators
  coating tungsten particles with dextran-conjugated, 181–182
  imaging *Xenopus* spinal neurons, 358, 361–364
  use in zebrafish, 51
Calcium phosphate transfection, of rat hippocampal neurons, 471
Calcium phosphate transfection buffer (recipe), 476
Calcium transients, imaging in *Xenopus* spinal neurons, 357–371
  advantages and limitations, 358
  imaging setup, 358
  overview, 357–358
  protocols
    imaging and analysis of *Xenopus* spinal neurons, 361–364
      data analysis, 364
      experimental method, 361–364
      imaging filopodial transients in vivo, 363–364, 364f
      imaging growth cone transients in vivo, 362–363, 363f
      materials, 361
      troubleshooting, 364
    perturbation of calcium dynamics in *Xenopus* spinal neurons, 365–368
      experimental method, 365–368
      imposition of Ca^{2+} spikes, 366–367, 366f
      manipulating filopodial Ca^{2+} dynamics, 368
      manipulating growth-cone Ca^{2+} dynamics, 367
      materials, 365
      suppresssion of Ca^{2+} transients, 365–366
      troubleshooting, 368
    preparation of *Xenopus* neuronal tissues for imaging, 359–360
      experimental method, 359–360
      materials, 359
      preparation of dissociated cell cultures, 359–360
      preparation of spinal cords, 360
      troubleshooting, 360
    recipes, 369–370
Cannibalism, minimizing, 514
Carbocyanine dyes
  ballistic labeling of developing retinal neurons
    applications, 187, 188f
    coating particles, 178–180, 179f
    shooting into tissue slices using gene gun, 185–186
  labeling of chick embryos, 91
  labeling second-order neurons in the posterior lateral-line (PLL) system (protocol), 285–287
  labeling *Xenopus* neurons for in vivo imaging, 388–389
  painting mouse embryos for imaging morphogenetic behavior and cell fates, 317–319
Carbon particles, labeling with, 582
Cardiovascular development, imaging mouse, 659–668
  confocal microscopy of vital fluorescent proteins, 660–663, 664f
    dynamic imaging of developing vasculature, 660–662, 661f
    hemodynamic analysis with fast-scanning confocal microscopy, 662–663, 664f
  optical coherence tomography (OCT) imaging, 664–667, 665f
    Doppler imaging of blood flow, 666–667
    experimental system, 664–666
    live structural imaging, 666
  overview, 659–660
CASK, 406
CAST/ERC, 406
Cautions, 855–862
Cdh16-Cre, 608
Cdh16-GFP, 608
CD-1 mice, 675, 676
Cdt1, 332
Cell contacts, visualizing in *Caenorhabditis elegans* embryos, 229–244
  overview, 229–230
  protocols
    acquisition of 4D DIC microscopic data to determine cell contacts, 235–238
      discussion, 238
      experimental method, 236–237
      imaging setup, 235
      materials, 236
      troubleshooting, 237–238
    agar mount preparation, 231–234
      agar pad preparation, 233f
      discussion, 234
      experimental method, 232–233

Cell contacts, visualizing in *Caenorhabditis elegans* embryos, (*Continued*)
imaging setup, 231
isolation of embryos and preparation for mounting, 232f
materials, 231
troubleshooting, 233–234
analysis of 4D DIC microscopic data to determine cell contacts, 239–240
discussion, 240
experimental method, 239–240
imaging setup, 239
materials, 239
troubleshooting, 240
laser killing of blastomeres, 241–242
discussion, 242
experimental method, 241–242
imaging setup, 241
materials, 241
troubleshooting, 242
recipes, 243
Cell-cycle progression, visualizing spatiotemporal dynamics of multicellular, 331–340
overview, 331–332
protocols
large-field high-resolution observation of tissue sections from Fucci mouse embryos, 337–339
experimental method, 338
imaging setup, 337
materials, 337
results and discussion, 338, 339f
long-term time-lapse imaging of NmuMG/Fucci2 cells, 333–336
experimental method, 335
imaging setup, 333, 334f
materials, 333–335
results and discussion, 335–336, 335f
Cell fate study, microinjection of Kaede mRNA for, 276–278, 277f
Cell membrane tagging, for imaging morphogenetic behavior and cell fates in mouse embryo, 317–319
Cell migration in chick explant cultures, 291–298
advantages and limitations, 297
application example, 296f, 297
overview, 291–292
preparation of chick explant cultures for imaging (protocol), 293–296
experimental method, 294–296
culture chamber preparation, 294–295
culture preparation, 295
embryo preparation, 295
microscope preparation, 294
microscope stage heater box assembly, 294
sagittal slice preparation, 295
imaging setup, 293
materials, 293
Cell movement, imaging in egg cylinder stage mouse embryos, 299–309
dissection of embryos, 304–306, 305f
example, 300f
overview, 299–301
protocol, 302–309
experimental method, 303–307
imaging setup, 302
materials, 302–303
recipes, 309
troubleshooting, 307–308
tissues of pregastrulation embryo, 299
transgenics for, 300–301
Cell polarity, visualizing in *Caenorhabditis elegans* embryos, 229–244
CellTrace BODIPY Texas Red (TR) methyl ester, 52, 57
Cerebral cortex
synaptic protein dynamics, imaging, 499–512
in vivo imaging of axonal and dendritic structures, 513–522
Cerl-GFP transgene, 300
Cerulean fluorescent protein
in Brainbow imaging, 192f, 194–196, 196f
use in BAPTISM, 251
c-fms promoter, 103, 103f
CFP. *See* Cyan fluorescent protein (CFP)
Channelrhodopsin, use in zebrafish, 51
Chapter guide, 4t–5t
Chick embryos
electroporation, 119–142
overview, 119–121
protocols
analysis of development following electroporation, 137
assembly of electrodes and wiring, 122–123, 122f
electroporation of chick limb mesoderm, 131–132
electroporation of chick neural tube, 126–128, 126f
electroporation of chick somatic mesoderm, 129–130
preparation of embryos, 124–125
troubleshooting, 138
high-resolution, multiphoton time-lapse imaging, 581–592
overview, 581–583
protocol, 584–590
assembly of imaging chamber and imaging, 588
discussion, 589–590
embryo electroporation and culture, 586
examples, 589f
experimental method, 584–588
imaging dish manufacture, 584–586, 585f, 586f, 587f
materials, 584
preparation of culture, 587–588
recipes, 590
live imaging, 85–99
advantages, 85–89
accessibility to fluorescent cell marking, 87f, 88–89
development in a planar volume, 87–88
imaging within egg or in culture chamber, 86f, 88
applications, 89–91
examples, 97
gastrulation, 89–90
neural crest cell migration, 90–91
cell labeling within the embryo, 91–92
electroporation of single- and multiple-colored DNA fluorescent proteins, 91–92
photoactivation of GFP variants, 87f, 92
transgenics, 92
viral labeling, 91
vital dye labeling, 91
embryo preparation (protocol), 93–97
egg preparation, 94
embryo placement in culture chamber, 96
imaging setup, 93
materials, 93
microscope preparation, 96
in ovo imaging preparation, 94
teflon membrane assembly, 94
whole-embryo culture preparation, 96
limitations, 87, 89
time-lapse imaging, 86f
microscopic magnetic resonance imaging (μMRI) of cardiac development, 792
Chick explant cultures, cell migration imaging in, 291–298
advantages and limitations, 297
application example, 296f, 297
overview, 291–292
preparation of chick explant cultures for imaging (protocol), 293–296
experimental method, 294–296
imaging setup, 293
materials, 293
Ciona intestinalis, 716–717, 817
Cited2, 786
Cited1-Cre, 609
Cleaning optical equipment, 835–836
Clearing, of *Xenopus embryos,* 733
CM-DiI, use in fate mapping, 312, 318f
Collagenase B, 359, 360
Collagenase solution (recipe), 643
Collagen gels, 639
Computed tomography (CT). *See* X-ray microtomography (microCT, μCT)
Confocal microscopy. *See also specific applications*
imaging cardiovascular development, 660–663, 664f
dynamic imaging of developing vasculature, 660–662, 661f
hemodynamic analysis with fast-scanning confocal microscopy, 662–663, 664f
line-scanning, 662
live imaging in zebrafish, 52
as nondestructive imaging, 740–741
preparation of fixed *Xenopus* embryos for imaging, 729–737
quantitative imaging of gene expression in *Drosophila melanogaster*, 689
Congenital heart defects, 647–648, 651, 652, 654
CoralHue (MBL International), 276
Cranial window, 514, 516–517
CreER driver, 206
CreERT2, 609
Cre/*loxP* system
genetic labeling of neurons in mouse brain, 203f, 204

Cre recombinase, 3
Brainbow imaging, 191, 194, 196–197
Cre-dependent adeno-associated virus preparation and delivery (protocol), 209–213
MADM, 165, 169–173
transgenic lines for cell movement imaging in egg cylinder stage mouse embryos, 301
transgenic mouse lines expressing in developing kidney, 608–609, 610t
Cre-X-Mice: A Database of Cre Transgenic Lines (website), 609
Cripto mouse mutant, 299
CT (computed tomography). *See* X-ray microtomography (microCT, μCT)
Culture medium (recipe), 488, 618
Cyan fluorescent protein (CFP)
axon labeling, 437, 438, 439, 440f, 447
use in zebrafish, 51
Cyclin E, 786
Cytomegalovirus (CMV), in Brainbow imaging, 194

D

Danieau's medium (30x) (recipe), 432, 432t
Danilchik's for Amy (DFA) medium (recipe), 566
DASPEI dyes, 284
Data volumes in multidimensional imaging, 596t
DBA/2J mice, 675, 678–679, 679f
Dechorionation
of *Drosophila*, 821
of zebrafish embryos, 257–258, 821
enzymatic, 257–258
manual, 257
Deconvolution software, 439
Dehydration of mouse embryo, 749–750
Dendra2, 92
Dendrites
simultaneous imaging of structural plasticity and calcium dynamics in developing, 479–489
overview, 479–480
protocol, 481–489
bolus labeling of neuronal structures, 483, 483f
confocal imaging, 485
discussion, 487
electrode preparation, 483
electroporation of individual cells, 484
experimental method, 482–486, 483f, 486f
hippocampal slice preparation, 482–483
image analysis, 484f, 485–486, 486f
imaging setup, 481
materials, 482
recipes, 488–489
troubleshooting, 486
simultaneous patch-clamping and calcium imaging in developing, 491–498
in vivo imaging in developing cortex in mice, 513–522
overview, 513–514
protocol, 515–521
application example, 520, 520f, 521f
discussion, 520–521
experimental method, 516–518
imaging setup, 515
materials, 515–516
troubleshooting, 518–519
in vivo time-lapse imaging of neuronal development in *Xenopus,* 387–404
DePex, 704
Depolarizing buffer (recipe), 476
Desflurane, for fly anesthesia, 38
Dextran-conjugated fluorescent dyes, for ballistic labeling of developing retinal neurons
coating particles, 181–182
shooting into tissue slices using gene gun, 185–186
DIASemb, 71
DiAsp dye, 282–284, 283f
Diazo-2AM, 367
Dicer2, 33
Dichroic beam splitter, 829f, 830
DiD
ballistic labeling of developing retinal neurons, 178–179
labeling *Xenopus* neurons for in vivo imaging, 388–389
Differential interference contrast (DIC) microscopy
imaging of epithelial morphogenesis, 631
live imaging of embryogenesis in *Caenorhabditis elegans,* 12, 12f
for visualizing cell contacts and cell polarity in *Caenorhabditis elegans* embryos, 230
acquisition of 4D DIC microscopic data (protocol), 235–238
discussion, 238
experimental method, 236–237
imaging setup, 235
materials, 236
troubleshooting, 237–238
agar mount preparation for observation of (protocol), 231–234
agar pad preparation, 233f
discussion, 234
experimental method, 232–233
imaging setup, 231
isolation of embryos and preparation for mounting, 232f
materials, 231
troubleshooting, 233–234
analysis of 4D DIC microscopic data (protocol), 239–240
discussion, 240
experimental method, 239–240
imaging setup, 239
materials, 239
troubleshooting, 240
laser killing of blastomeres (protocol), 241–242
discussion, 242
experimental method, 241–242
imaging setup, 241
materials, 241
troubleshooting, 242
Diffuse optical tomography (DOT), 741
Diffusion tensor imaging (DTI), 792–793, 793f
Digital scanned laser light-sheet fluorescence microscopy (DSLM), 815–825
imaging of zebrafish and *Drosophila* development (protocol), 818f
experimental method, 821–824
imaging setup, 819
materials, 820–821
principles, 815–817, 816f
reconstructing cell behavior from recordings, 819f
sample preparation for whole-embryo imaging, 818f
setup, 818f
DiI
axon pathfinding in *Xenopus,* 373
ballistic labeling of developing retinal neurons, 178–179
cell movement imaging in egg cylinder stage mouse embryos, 300
labeling second-order neurons in the posterior lateral-line (PLL) system (protocol), 285–287
labeling *Xenopus* neurons for in vivo imaging, 388–389, 393–398
vital dye labeling of chick embryos, 91
DiO
ballistic labeling of developing retinal neurons, 178–179
labeling *Xenopus* neurons for in vivo imaging, 388–389
painting mouse embryos for imaging morphogenetic behavior and cell fates, 317–319, 318f
use in fate mapping, 312
Dissection medium (recipe), 510
Divalent-cation-free medium (recipe), 369
DNA
ballistic labeling of developing retinal neurons
coating gold particles with DNA, 183–184
shooting into tissue slices using gene gun, 185–186
electroporation of chick and mouse embryos, 119–142
electroporation of mouse embryos, 323–326
endotoxin-free plasmid DNA, 147
preparation for electroporation, 121
single-cell electroporation (SCE) of DNA for neuronal transfection in *Xenopus,* 146–147, 149–153
in *Xenopus,* 146–147, 149–153, 389, 390f
DNA microinjection in zebrafish, 51
constructing a microinjection chamber for eggs, 56
DNA injection into early embryos, 411–412
DNA injection to generate transiently transgenic retinal progenitor cells, 260
protocol, 53–55, 54f
DNA solution for injection (recipe), 64
Doppler imaging of blood flow, 666–667
DOT (diffuse optical tomography), 741
Double-stranded RNA (dsRNA) electroporation in chick embryos, 120
Dpp (Decapentaplegic), 29, 535f, 536, 538–543, 548
DR75 (recipe), 328

Drosophila melanogaster
advantages of working with, 23–24
anesthetizing, 38
bicoid morphogen gradient, quantifying, 523–532
experimental procedures
antibody staining, linearity of, 526, 527f
calculating absolute bicoid concentration, 528–529, 528f, 529f
fly strain generation, 525–526
imaging of live embryos, 526, 528
microscopy apparatus, 524–525, 524–530, 525f
quantification of errors, 530
reproducibility across embryos, measuring, 529–530
overview, 523–524, 530–531
digital scanned laser light-sheet fluorescence microscopy (DSLM), 820–823
ease of genetic manipulation in, 24
gene expression, quantitative imaging of, 683–697
confocal microscopy, 689
image and data processing methods, 689–695
background removal, 691–693, 692f
data averaging, 694–695, 695f
image registration, 694
image segmentation, 689–691
temporal characterization of embryos, 693–694
method overview, 684, 685f
overview, 683–684
preparation of embryos (protocol), 686–688
embryo collection and fixation, 687
immunostaining, 687–688
materials, 686–687
troubleshooting, 688
recipes, 696
gene expression mapping for blastoderm, 699–710
pipeline, 703–707
conversion of images to point clouds, 704–706, 705f
PointCloudXplore visualization tool, 706–707, 708f
registration of point clouds into a virtual embryo, 706, 707f
staining, mounting, and imaging, 703–704
temporal staging, 704
strategy, 700–703
high-throughput imaging and analysis, 702–703
pattern dynamics, 701–702
genetic resources for, 31t
genome, 24
life cycle, 25f
live imaging, 23–48
applications, 24–29
in adults, 28
advanced, 29
in embryos, 25–26
imaging modality, choice of, 24
in larvae, 26
overview, 24
in pupae, 28
dissecting and mounting, general considerations in, 33–34
genetic tools to prepare for imaging, 29–33
fluorescent transgenes, 29, 31
mutants, 33
transgene expression, 31–32
transgenic lines of interest, 30t
transgenics, 32–33
of imaginal discs, 26
neuroblast lineages within intact larval brains, 217–227
overview, 217–219, 218f, 218t, 219t, 225
protocol, 220–224
protocols, 35–43
dissection of ovaries from adults for imaging in halocarbon oil, 41–42
imaging pupae using window method, 39–40
mounting embryos in halocarbon oil, 35–36
obtaining staged larvae for live-imaging experiments, 37–38
recipes, 43
reagents commonly used in, 27t–28t
MARCAM (mosaic analysis with a repressible cell marker)
examples of applications, 158f, 162–164
analysis of neuronal morphogenesis, 163–164, 164f
live imaging, 163
tracing neural circuits, 162–163
principle, 159–160, 160f
protocol, 166–168
morphogen gradients in imaginal discs, quantitative imaging of, 533–550
measuring kinetic parameters of morphogen spreading using FRAP, 538–542, 539f
bleaching depth and photodamage, 540
choice of region of interest, 540–541
detection sensitivity, 541
intracellular and extracellular pools, 542
photobleaching during image acquisition, 541
theoretical analysis of FRAP experiments, 541–542
tissue geometry and subcellular morphogen distribution, 539–540
measuring shape of, 534–538, 535f
calibrating fluorescence intensity to molecular number, 537
imaging in linear range of detection, 536–537
quantifying gradient shape, 537–538
measuring subcellular morphogen dynamics using particle tracking, 542–547
parameters of endosomal dynamics, 546–547
particle detection, 543, 544f, 545
particle tracking, 544f, 545–546
neuroblast lineage imaging within intact larval brains in *Drosophila*, 217–227
overview, 217–219
example studies, 218–219, 218f
fusion lines, 218t
neuroblast Gal4 driver lines, 219t
protocol, 220–224
image acquisition, 223
imaging setup, 220, 221f
larval dissection, 221–222
materials, 220–221
recipes, 225
specimen orientation and slide sealing, 222
troubleshooting, 223–224
resources for live imaging
genetic, 841t
reagents, 837t–838t
recipes, 838–839
transgenic lines, 840t–841t
sex determination in, 24
stock centers, 24
DSLM. *See* Digital scanned laser light-sheet fluorescence microscopy (DSLM)
DTI (diffusion tensor imaging), 792–793, 793f
dTomato, in Brainbow imaging, 192f, 194–196, 196f
Dynamic imaging of developing vasculature, 660–661, 661f

E

E3 buffer (recipe), 414
ECM (extracellular matrix), 624–626
Edinburgh Mouse Atlas Gene Expression Database, 751
Edinburgh Mouse Atlas Project (EMAP), 794, 795
E3 embryo medium (60x) (recipe), 385
EFIC. *See* Episcopic fluorescence image capturing (EFIC)
eGFP. *See* Enhanced green fluorescent protein (eGFP)
Egg cylinder stage mouse embryos
cell movement imaging in, 299–309
example, 300f
overview, 299–301
protocol, 302–309
experimental method, 303–307
imaging setup, 302
materials, 302–303
recipes, 309
troubleshooting, 307–308
transgenics for, 300–301
dissection of, 304–306, 305f
tissues of pregastrulation, 299
Electromagnetic pulse (EMP), 834
Electromagnetic spectrum, 827, 828f
Electroporation
advantages of, 139–140
applications, 140
basics/principles of, 120, 144
bulk electroporation of RGCs or CNS neurons in live *Xenopus* tadpoles, 399–402, 401f
cell-specific promoters, use of, 140
chick embryos, 119–142
of living embryos, 91–92
overview, 119–121
protocols
analysis of development following electroporation, 137

assembly of electrodes and wiring, 122–123, 122f
electroporation of chick limb mesoderm, 131–132
electroporation of chick neural tube, 126–128, 126f
electroporation of chick somatic mesoderm, 129–130
preparation of embryos, 124–125
troubleshooting, 138
considerations when performing, 120–121
description, 3
examples, 139, 139f
limitations of, 140
lipofection as alternative to, 140
making zebrafish mosaic primordia by focal electroporation, 279–281, 280f
mouse embryos, 119–142
advantages and disadvantages of, 327
overview, 119–121
protocols
analysis of development following electroporation, 137
assembly of electrodes and wiring, 122–123, 122f
electroporation method, 136
marking cells for imaging morphogenetic behavior and cell fates, 323–326
preparation of culture medium, 133–134
preparation of embryos, 135
troubleshooting, 138
staging and electroporation parameters, 134t
in utero, 138
nucleofection, 454
of rat hippocampal neurons, 483f, 484
single-cell electroporation (SCE), 138
of rat hippocampal neurons, 483f, 484
in *Xenopus,* 143–155, 389, 390f
efficiency, factors influencing, 144–146
electroporation of tadpole tectal neurons (protocol), 149–154
implementation, 146–148
labeling individual neurons in the brains of live tadpoles by electroporation of dyes or DNA (protocol), 393–395
overview, 143, 144
setup, 145f
targeted delivery in living avian embryos, 91–92
in zebrafish, 52
Embedding agarose (recipe), 415
Embedding embryos for microCT, 757–759
procedure A (most embryos), 757–758, 757f
procedure B (early chick embryos), 757–758, 758f, 759f
procedure C (for resin-embedded samples for subsequent sectioning), 759
Embryo embedding agar (recipe), 385
Embryo embedding agarose (recipe), 267
Embryo glue (recipe), 43
Embryo medium (E3M) (60x stock solution) (recipe), 268
Embryo medium (recipe), 64, 578
Embryo time-lapse solution (recipe), 268
E3 medium (60x stock) (recipe), 824
Emission filter, 829–830, 829f
Emission fingerprinting, 439
Emission maxima, for fluorochromes, 831t–832t
EMP (electromagnetic pulse), 834
Endosome localization and tracking, 544f, 546–547
Enhanced green fluorescent protein (eGFP)
for cotransfection of rat hippocampal neurons, 469, 473f
electroporation, 139, 139f
in genetic labeling of neurons in *Xenopus,* 390f, 401–402
Hoxb7/eGFP strains, 607–608, 607f, 607t
time-lapse imaging of fluorescently labeled live cells in embryonic mammalian forebrain, 342
use in *Drosophila*, 31
Enhanced yellow fluorescent protein (eYFP)
dynamic imaging of developing vasculature, 660–661, 661f
Eos fluorescent protein (EosFP), 29
Epiblast cells, movement of, 299–300
Episcopic fluorescence image capturing (EFIC), 765
applications of, 766
description of, 766–767
embedding samples for EFIC imaging, 771–772
example, 767f
generation of volume data, 775
Episcopic three-dimensional imaging of embryos, 765–776
applications of, 766
imaging equipment, 768–770, 769f
digital camera, 770
filter cubes, 770
microtome, 768, 770
overview, 766–768
protocols
embedding samples for EFIC imaging, 771–772
embedding samples for HREM imaging, 773–774
generation of volume data, 775
Epithelial morphogenesis, long-term imaging on three-dimensional organotypic cultures, 623–645
bringing sample to microscope stage (practical), 631–633, 633f
bringing sample to microscope stage (theory), 629–631
environmental control, 633–639, 634f
isolation of mouse mammary organoids for long-term time-lapse imaging (protocol), 640–643
limiting phototoxicity and photobleaching, 628–629
microscopic requirement issues, 626–628
overview, 623–625, 624f
common features, 625
culture models for, 624–625, 625f
temperature issues, 633–637
ε-globin
ε-globin-GFP for hemodynamic analysis in yolk sac, 663, 664f
promoter, 103, 103f, 104
Ether, for fly anesthesia, 38
Excitation filter, 829, 829f
Excitation maxima, for fluorochromes, 831t–832t
Explants
cell migration imaging in chick, 291–298
advantages and limitations, 297
application example, 296f, 297
overview, 291–292
preparation of chick explant cultures for imaging (protocol), 293–296
experimental method, 294–296
imaging setup, 293
materials, 293
imaging of mouse retinal whole mounts, 419–425
discussion, 424
examples, 424, 425f
experimental method, 421–423
image acquisition, 422–423
imaging setup, 419–420
labeling, 422
materials, 420–421, 421f
mounting, 422
retinal explant preparation, 421–422
troubleshooting, 423–424
microsurgical approaches to isolate cells and tissues in *Xenopus* (protocol), 555–557
experimental method, 555–557, 557
animal cap explant, 556
general procedures, 555–556
marginal zone explant, 556
"windowed" embryo, 556–557
materials, 555
Expression profiling in *Caenorhabditis elegans* embryos, 799–814
External solution (recipe), 497
Extracellular matrix (ECM), 624–626
Eye development
micro-ultrasound imaging
of normal ocular development
ocular microcirculation, 677, 677f
primary ocular tissues, 676, 676f
ocular disease models, 678–679
glaucoma, 678–679, 679f
retinoblastoma, 678, 678f
procedures for imaging of mice (protocol), 673–675
retinal circuits, imaging of, 417–434
general imaging considerations, 418
overview, 417–418
protocols, 419–433
in vitro imaging of retinal whole mounts, 419–425
in vivo imaging of zebrafish retina, 416–431
retinal neurons, ballistic labeling of developing, 177–190
retinal progenitor lineages in developing zebrafish retina, imaging, 253–268
imaging setup, 254–255
overview, 253–254, 267
protocols
DNA injection to generate transiently transgenic retinal progenitor cells, 260
embedding embryos, imaging, staining, and image processing of developing zebrafish retina, 261–267

Eye development (*Continued*)
recipes, 267–268
transplantation of transgenic progenitor retinal cells expressing fluorescent markers, 256–259

F

Fast Green, 398
Fate mapping by grafting, 582
Favia favus, 92
Fibronectin-conjugated polyacrylamide gel (FN-PAG), 558–559
Filters, fluorescence microscopy, 829–830, 829f
Fixation buffer (recipe), 696
Fixative solution (recipe), 476
Fix solution (recipe), 728
Flippase (FLP)/flippase recognition target (FRT) system
MARCAM (mosaic analysis with a repressible cell marker), 159, 160f, 162, 166–168
use in *Drosophila*, 33, 159, 160f
Flk1 promoter, 103, 103f, 104
Flna, 786
Fluo-3AM indicator, 361, 363, 367
Fluo-4AM indicator, 361–364, 367
Fluo-3AM or Fluo-4AM (recipe), 369
Fluo-3 indicator, 358, 361, 364, 368
Fluo-4 indicator, 358, 361, 363, 364, 368
Fluorecence intensity, calibrating to molecule number, 537
Fluorescein, caged, 277
Fluorescence microscopy. *See also specific applications*
live imaging of embryos
in *Caenorhabditis elegans*
phototoxicity, 13
signal loss issues, 13
temperature control, 13–14
in chick, 88–89
in mouse, 103–104, 103f
safe operation of fluoresence microscope, 833
Fluorescence microscopy filters, 829–830, 829f
Fluorescent dextrans
for ballistic labeling of developing retinal neurons, 181–182, 185–186
labeling *Xenopus* neurons for in vivo imaging, 388, 393–398
Fluorescent dyes
ballistic labeling of developing retinal neurons
coating tungsten particles with dextran-conjugated, 181–182
shooting into tissue slices using gene gun, 185–186
electroporation and
in living chick embryos, 91–92
single-cell electroporation (SCE) in *Xenopus,* 147–148, 147f, 393–395
labeling hair cells and afferent neurons in the posterior lateral-line (PLL) system (protocol), 282–284
Fluorescent labeling
time-lapse imaging of fluorescently labeled live cells in embryonic mammalian forebrain, 341–355
time-lapse imaging of neuronal development in *Xenopus,* 387–404
in zebrafish, 51–52
Fluorescent proteins
in Brainbow imaging in zebrafish, 191–197
fusions useful as markers of synaptic components, 470t
imaging cardiovascular development, 660–663, 664f
dynamic imaging of developing vasculature, 660–662, 661f
hemodynamic analysis with fast-scanning confocal microscopy, 662–663, 664f
kidney expression of in transgenic mouse lines, 607–608, 607f, 607t
photoactivatable (PAFPs)
use in *Drosophila,* 29–31
use in living chick embryo, 87f, 89, 92
use in zebrafish, 51
photoconvertable
Kaede use in birthdating in zebrafish, 245–250, 246f, 247f
Kaede use in labeling defined cells in zebrafish embryos, 276–278, 277f
KikGR use in cell movement imaging in egg cylinder stage mouse embryos, 300f, 301
sample preparation for using live reporters (protocol), 553–554
coexpression of multiple reporters, 554
experimental method, 553–554
generation of embryos with evenly distributed expression of reporter, 554
generation of embryos with mosaic expression of reporter, 554
material, 553
mRNA synthesis, 553
targeted microinjection on mRNA encoding fluorescent proteins in *Xenopus,* 73, 74f
use in zebrafish, 51, 53–55
Fluorescent recovery after photobleaching. *See* FRAP (fluorescent recovery after photobleaching)
Fluorochromes
emission maxima, 831t–832t
excitation maxima, 831t–832t
Fluorophores
for quail development imaging, 595
use in *Drosophila*, 29, 30t, 31
Fluoro-Ruby, 187, 188f
FlyBase, 33
FlyTrap, 31
FM1-43 dye, 284
Focal electroporation, making zebrafish mosaic primordia by, 279–281, 280f
Fomblin, 794
Four-dimensional (4D) imaging
cell contact visualization in *Caenorhabditis elegans* embryos
acquisition of 4D DIC microscopic data to determine cell contacts (protocol), 235–238
discussion, 238
experimental method, 236–237
imaging setup, 235
materials, 236
troubleshooting, 237–238
analysis of 4D DIC microscopic data to determine cell contacts (protocol), 239–240
discussion, 240
experimental method, 239–240
imaging setup, 239
materials, 239
troubleshooting, 240
optical coherence tomography (OCT) of beating embryonic heart, 650–655
quail development, fluorescent imaging of
4D fluorescent imaging of quail embryos (protocol), 597–604
experimental method, 598–602
imaging setup, 597
materials, 597–598
recipe, 604
troubleshooting, 602–603
retinal progenitor lineages in developing zebrafish retina, imaging, 253–268
imaging setup, 254–255
acquisition, 254
processing, 255
overview, 253–254, 267
protocols
DNA injection to generate transiently transgenic retinal progenitor cells, 260
embedding embryos, imaging, staining, and image processing of developing zebrafish retina, 261–267
recipes, 267–268
transplantation of transgenic progenitor retinal cells expressing fluorescent markers, 256–259
4F1G (recipe), 763
Fourier domain mode-locked (FDML) laser, use with optical coherence tomography, 652, 652f, 653f
FRAP (fluorescent recovery after photobleaching)
measuring kinetic parameters of morphogen spreading, 538–542, 539f
bleaching depth and photodamage, 540
choice of region of interest, 540–541
detection sensitivity, 541
intracellular and extracellular pools, 542
photobleaching during image acquisition, 541
theoretical analysis of FRAP experiments, 541–542
tissue geometry and subcellular morphogen distribution, 539–540
synaptic protein dynamics, imaging, 499–500
Frequency, 827
Frizzled, 743
Fucci
description, 332
as fluorescent ubiquitination-based cell-cycle indicator, 332
imaging setup for observing, 333, 334f
large-field high-resolution observation of tissue sections from Fucci mouse embryos, 337–339
long-term time-lapse imaging of NmuMG/Fucci2 cells, 333–336
schematic structure of, 332f
Fucci2 probe
description, 332

imaging setup for observing, 333, 334f
long-term time-lapse imaging of NmuMG/Fucci2 cells, 333–336
schematic structure of, 332f
Fura-2AM indicator, 361–362
Fura-2 indicator, 358
Fura Red-AM indicator, 363
Fusion proteins
bicoid-green fluorescent protein (Bcd-GFP), 525–526, 528–529, 528f, 529f
GFP-fusion proteins, in *Xenopus* embryo live imaging, 82

G

$GABA_A$ receptor δ, 206
GAD67-GFP transgenic mouse, 424, 425f
GAL80, use in *Drosophila,* 159–160, 160f
Gal4 transcriptional activator, 32, 159, 219t
Gal4-UAS system
use in *Drosophila*, 32, 159–160, 160f, 162, 166–168
for neuroblast lineage imaging within intact larval brains, 217–219, 218t, 219t, 225
use in genetic labeling of neurons in mouse brain, 204
use in zebrafish, 62, 407–408
Gastrulation
in *Drosophila* embryos, 26
live imaging in chick embryos, 89–90
GCaMP, 29
Geminin, 332
Gene expression, quantitative imaging of in *Drosophila,* 683–697
confocal microscopy, 689
image and data processing methods, 689–695
background removal, 691–693, 692f
data averaging, 694–695, 695f
image registration, 694
extraction of ground control points, 694
image segmentation, 689–691
acquisition of quantitative data, 690, 690f
construction of nuclear mask, 690
one-dimensional expression patterns, 691, 691f
rotation of images to standard orientation, 689–690, 690f
temporal characterization of embryos, 693–694
prediction of developmental age, 693–694
temporal classification, 693
method overview, 684, 685f
overview, 683–684
preparation of embryos (protocol), 686–688
embryo collection and fixation, 687
immunostaining, 687–688
materials, 686–687
troubleshooting, 688
recipes, 696
Gene expression mapping for *Drosophila* blastoderm, 699–710
pipeline, 703–707
conversion of images to point clouds, 704–706, 705f
PointCloudXplore visualization tool, 706–707, 708f
registration of point clouds into a virtual embryo, 706, 707f
staining, mounting, and imaging, 703–704
temporal staging, 704
strategy, 700–703
high-throughput imaging and analysis, 702–703
pattern dynamics, 701–702
Gene Expression Nervous System Atlas (GENSAT), 608
Gene expression patterns, analyzing with optical projection tomography (OPT), 743–744
Gene gun, for ballistic labeling of developing retinal neurons, 177–189
applications, 187
coating particles
with carbocyanine dyes, 178–180, 179f
with dextran-conjugated fluorescent dyes, 181–182
with DNA, 183–184
depth of labeling, 187
protocol for use of gene gun, 185–186
tissue damage, 187
Gene targeting in mice
genetic labeling of neurons in brain, 202–203, 202f, 208
Genetic labeling by fluorescent protein expression in *Xenopus,* 389–390
Genetic labeling of neurons in mouse brain, 199–216
achieving robust and specific neuron labeling, 204–206
Cre/*loxP* system, 204
driver alleles, technical tips on, 206
transcription activation system, 204
transgenic overexpression, 206
viruses as reporter components in binary systems, 205–206, 205f
binary expression systems
Cre/*loxP* system, 203f, 204
direct labeling compared, 208
gene targeting and, 202–203, 202f, 203f
viruses as reporters in, 205–206, 205f
Cre-dependent adeno-associated virus preparation and delivery (protocol), 209–213
AAV delivery, 211–212
AAV production and serotypes, 211
imaging setup, 209
materials, 209–210
troubleshooting, 212–213
viral vector design, 210–211
overview, 199
relative merits of methods, 208
binary system versus direct labeling, 208
expression levels, 208
gene targeting versus transgenesis, 208
specificity and reliability of cell labeling, 200–202
gene targeting approach, 201f, 202
transgenic approach, 200–202, 201f
strategies
Brainbow, 207
intersectional recombination, specificity increase through, 206–207, 207f
mosaic analysis with double markers, 207
single-neuron labeling with inducible Cre-mediated knockout (SLICK), 207
Genetic methods
methodological categories, 157
single-neuron labeling using, 157–175
GenitoUrinary Development Molecular Anatomy Project, 608
GFP. *See* Green fluorescent protein (GFP)
GFP-Dpp (Decapentaplegic), 535f, 538–543, 546
GFP-fusion proteins, in *Xenopus* embryo live imaging, 82
Glass micropipettes, in single-cell electroporation (SCE) in *Xenopus,* 144–145
Glaucoma, 675
Glossary, 845–853
Gold particles, coating with DNA, 183–184
Golgi, Camillo, 157
Golgi staining, 157, 159, 164–165
Grafting
cells into mouse embryo (protocol), 320–322
experimental method, 321–322, 322f
materials, 320
troubleshooting, 322
fate mapping by, 582
Grape juice agar (recipe), 696
Gräper, Ludwig, 581
Green fluorescent protein (GFP)
bicoid-green fluorescent protein (Bcd-GFP), 525–526, 528–530, 528f, 529f
fluorescent transgene expression in mouse embryos, 103, 103f, 104
in genetic labeling of neurons
in mouse brain, 200, 201f, 202f, 203f, 204, 205f
in *Xenopus,* 389, 390f, 395
GFP-Dpp (Decapentaplegic) fusion, 535f, 538–543, 546
hippocampal neurons in culture, imaging, 450, 455, 459f, 460, 461, 462f463
imaging synaptogenesis in *Xenopus,* 406–414, 407f–409f
kidney expression of in transgenic mouse lines, 607–608, 607f, 607t
in live imaging of *C. elegans,* 12–13
membrane tagged (memGFP), 82
morphogen fusions, 535f, 536, 538–543, 546
myristoylated variant of, 608
photoactivation
in *Drosophila*, 29
in imaging synaptic protein dynamics, 500, 506–509, 508f
in live avian embryos, 92
in *Xenopus,* 401–402, 401f
photobleaching, 530
retinal development imaging in zebrafish, 254, 256, 260
in *Xenopus* embryo live imaging, 82, 401–402, 401f
in zebrafish, 51
GTPases
Rac, 163
Rho, 163
Guide to chapters, 4t–5t

H

Hair cells of lateral-line system
function, 271–272
labeling, 282–283, 283f, 284

Halocarbon oil, 33–34, 35–36, 41–42
Halorhodopsin, use in zebrafish, 51
Hazardous materials, 857–861
Heart
  congenital defects, 647–648, 651, 652, 654
  looping stage of development, 648–649
  microscopic magnetic resonance imaging (μMRI) of avian cardiac development, 792
  optical coherence tomography (OCT) imaging, 647–655
    of early quail heart (protocol), 655
    methods and results, 650–654, 651f–654f
    overview, 649–650
Heated microscope enclosures, 636–637
Heater
  objective lens, 635–636
  sample chamber, 635
Heater box/chamber, 88, 105, 105f, 106f
Heat filter, 830
Heat shock promoter, in Brainbow imaging, 194
Heat-shock-protein 70 (hsp70) promoter, 32, 159
Helios Gene Gun (Bio-Rad Laboratories), 177, 179f, 187
Hemodynamic analysis with fast-scanning confocal microscopy, 662–663, 664f
Hex-GFP transgene, 300
Hex-Venus transgene, 300
High-resolution, multiphoton time-lapse imaging of early chick embryos, 581–592
High-resolution episcopic microscopy (HREM), 765
  applications of, 766
  description, 766–768
  embedding samples for HREM imaging, 773–774
  example, 767f, 769f
  generation of volume data, 775
  imaging equipment, 768–770, 769f
High-throughput imaging and analysis
  for creation of computationally analyzable gene expression atlas, 702–703
  of mouse embryos by magnetic resonance imaging, 777–787
Hippocampal neurons in culture, imaging, 449–465
  general imaging considerations, 450–454
    cameras, 452
    environmental control, 453–454, 453f
    imaging modalities, 450–451
    labeling cells with GFP-tagged proteins, 454
    microscope configuration and automation, 452
    objectives, 452
  overview, 449–450, 451f
  protocols
    long-term time-lapse imaging, 455–459
      examples, 458, 458f, 459f
      image acquisition, 457
      labeling cells by nucleofection, 456
      materials, 455
      method, 456–457
      mounting coverslips for imaging, 456–457
      troubleshooting, 457–458
    short-term high-resolution imaging with rapid image acquisition, 460–463
      discussion, 463
      examples, 461–462, 462f
      image acquisition, 461
      labeling cells by lipid-mediated transfection, 460–461
      materials, 460
      method, 460–461
      troubleshooting, 461
Histo-Clear (National Diagnostics), 771–772
HL3 solution (recipe), 838
  zero-calcium, 839
Holtfreter buffer (recipe), 268
Hoxb7-Cre, 609
Hoxb7/eGFP strain, 607–608, 607f, 607t
Hoxb7/myr-Venus strain, 608
Hoxb7/rtTA strain, 608
HREM. *See* High-resolution episcopic microscopy (HREM)
HuC promoter, use in birthdating in zebrafish, 245, 248–250

I

Ifitm1 and *Ifitm3* genes, 327
ImageJ software (NIH), 274, 420, 481, 565, 595, 718
Image processing and analysis, 563–565
  kymographs, 563, 563f
  managing your region of interest, 565
  projecting images, 564–565, 564f
Imaginal discs, 26, 38
  morphogen gradient, quantitative imaging of
    measuring kinetic parameters of morphogen spreading using FRAP, 538–542, 539f
      bleaching depth and photodamage, 540
      choice of region of interest, 540–541
      detection sensitivity, 541
      intracellular and extracellular pools, 542
      photobleaching during image acquisition, 541
      theoretical analysis of FRAP experiments, 541–542
      tissue geometry and subcellular morphogen distribution, 539–540
    measuring shape of, 534–538, 535f
      calibrating fluorescence intensity to molecular number, 537
      imaging in linear range of detection, 536–537
      quantifying gradient shape, 537–538
    measuring subcellular morphogen dynamics using particle tracking, 542–547
      parameters of endosomal dynamics, 546–547
      particle detection, 543, 544f, 545
      particle tracking, 544f, 545–546
Imaris software (Bitplane), 114, 420, 594–595
Immunocytochemistry, imaging synapse formation and function in neuronal cell cultures by quantitative, 468–476
  discussion, 475
  experimental method, 469–474
    assay of synaptic function at single synapse level, 471–472
    image analysis, 472–474, 473f, 474f
    immunostaining and image acquisition, 472
    neuronal cell culture, 469
    transfection, 469–471
  imaging setup, 468
  materials, 468–469
  recipes, 476
  troubleshooting, 474–475
Immunohistochemistry, optical projection tomography (OPT) and, 745–746
Immunostaining, 472, 687–688
Incubator, stage-top, 637
In ovo imaging of chick embryos, 86f, 88, 94, 95f
In situ hybridization
  optical projection tomography (OPT), 746
  whole-mount in situ hybridization (WMISH), 743, 746
Instars, *Drosophila,* 26
Intensity footprint of fluorescent particles, 543
Internal solution (recipe), 497
Intersectional recombination, 206, 207f
Intravital dyes, use in zebrafish, 52, 57
Ion indicators
  coating tungsten particles with dextran-conjugated, 181–182
Ionophoresis
  dye labeling retinal ganglion cell axons in live *Xenopus* tadpoles, 396–398, 398f
IPLab, 274
Iridophores, zebrafish, 50
ISce1 meganuclease, 260
Islet1 gene, 196f, 197
Isoflurane, for anesthesia in mice, 516, 673

J

JB-4 resin embedding kit (Polysciences, Inc.), 773–774
jEdit, 718
JTree, 805
Jupiter gene, G147 as protein trap in, 225

K

Kaede, 51, 92
  birthdating in zebrafish, 245–250, 246f, 247f
  labeling defined cells or subsets of cells in zebrafish embryos, 276–278, 277f
Kidney development, imaging, 605–621
  dissecting of embryonic mouse kidney, culture in vitro, and imaging of the developing organ (protocol), 611–618
    experimental method, 612–616
      dissection of fetal mouse kidney, 612–614, 613f
      imaging kidney development in culture, 615–616, 615f, 616f
      isolation of ureteric bud and metanephric mesenchyme, 614–615
    imaging setup, 612, 612f
    materials, 611–612
    recipe, 618
    troubleshooting, 616–617
  overview, 605–606
  transgenic mouse lines, 607–610

lines expressing Cre recombinase, 608–609, 610t
lines expressing fluorescent proteins, 607–608, 607t
KikGR, 51, 87f, 92, 300f, 301
Kinesin motor dynamics in stage 2 neurons, 458, 459f
Ksp-cadherin, 608
KusabiraOrange2 (KO2), in Fucci probe, 332, 332f
Kymographs, 563, 563f
Kynurenic acid stock solution (100 mM) (recipe), 488

L

LacZ expression in mouse embryo, 744–745, 744f
LAS AF software, 689
Laser Doppler velocimetry (LDV), 651–652, 651f, 653
Laser killing of *Caenorhabditis elegans* blastomeres (protocol), 241–242
discussion, 242
experimental method, 241–242
imaging setup, 241
materials, 241
troubleshooting, 242
Lasers, safe operation of, 833–834
Lateral-line system
anatomy of, 271–272
development of, 272
imaging development of, 271–289
labeling defined cells or subsets of cells by Kaede photoconversion (protocol), 276–278
discussion, 277–278
injecting Kaede mRNA for cell fate studies, 276
Kaede photoconversion, 277, 277f
materials, 276
labeling hair cells and afferent neurons in the posterior lateral-line (PLL) system (protocol), 282–284
afferent neuron labeling, 283–284, 283f
discussion, 284
hair cell labeling, 282–283, 283f
materials, 282
labeling second-order neurons in the posterior lateral-line (PLL) system (protocol), 285–287
discussion, 286–287
materials, 285
method, 286
troubleshooting, 286
making mosaic primordia by focal electroporation (protocol), 279–281
discussion, 280–281
materials, 279
method, 279–280, 280f
time-lapse analysis of primordium migration (protocol), 273–275
discussion, 274–275
materials, 273–274
method, 274
motorization, 275
mounting medium, 274
troubleshooting, 274
innervation of, 271–272
Lefty-DsRed2 transgene, 300
lexA/lexAO system
use in MARCAM (mosaic analysis with a repressible cell marker), 159–160
LHβTAg mice, 675, 678, 678f
Light-gated glutamine receptor (LiGluR), 51
Light-sheet-based fluorescence microscopy (LSFM), 815–817, 816f
Lineage tracking, of retinal progenitor lineages in developing zebrafish retina, 253–268
imaging setup, 254–255
acquisition, 254
processing, 255
overview, 253–254, 267
protocols
DNA injection to generate transiently transgenic retinal progenitor cells, 260
embedding embryos, imaging, staining, and image processing of developing zebrafish retina, 261–267
recipes, 267–268
transplantation of transgenic progenitor retinal cells expressing fluorescent markers, 256–259
Lipid-mediated transfection, 460–461
Lipofectamine 2000, 460–461
transfection of rat hippocampal neurons, 469–471
Lipofection, 460
electroporation as alternative to, 140
Lipophilic dyes
labeling of chick embryos, 91
labeling *Xenopus* neurons for in vivo imaging, 388–389, 393–398
optical projection tomography (OPT), 746
for tracing axons and cell movements, 746
Lis1, 164
Lissencephaly, 164
Live imaging. *See also specific applications*
in Drosophila, 23–48, 163
neuroblast lineages within intact larval brains, 217–227
resources for
genetic, 841t
reagents, 837t–838t
recipes, 838–839
transgenic lines, 840t–841t
in embryos
avian, 85–99
Caenorhabditis elegans, 11–21
mouse, 101–117
Xenopus, 69–84
zebrafish, 49–68
overview of live cell imaging, 2–6
cell fate, differentiation, and migration, 3–6
imaging circuit formation, 6
labeling cells, 3
single-neuron labeling using genetic methods, 163
LNL-GFP, 401f, 402
Low-melting-point agarose (recipe), 432
LoxP, 165, 192f
LSFM (light-sheet-based fluorescence microscopy), 815–817, 816f
Luteinizing hormone β subunit T-antigen (LHβTAg), 675, 678, 678f

M

MADM (mosaic analysis with double markers), 3
genetic labeling of neurons in mouse brain, 207
MARCAM (mosaic analysis with a repressible cell marker) compared to, 161–162
principle of, 160–162, 161f
protocol in mice, 169–173
equipment, 169
experimental method, 170–171
imaging setup, 169
materials, 169
troubleshooting, 171–172
ROSA26 and, 169–171
Magnetic resonance imaging (MRI)
in developmental biology, 789–798
advantages of MRI, 789–790
resolution, 790
signal-to-noise ratio, 790
when to use MRI, 790
high-throughput analysis of mouse embryos, 777–787
overview, 777–778
protocol, 779–787
data reconstruction and analysis, 782–785, 783f, 784f
discussion, 786
embryo preparation, 780–782
experimental method, 780–785
imaging setup, 779
materials, 779–780
recipes, 786–787
troubleshooting, 785
microscopic magnetic resonance imaging (μMRI), 740
developmental atlas, 793–797
labeling anatomy, 794–795, 796f
mouse, 794
quail, 794, 795f
visualizing developing anatomy from atlases, 796–797
live imaging
amphibian development, 791–792, 791f
avian cardiac development, 792
diffusion tensor imaging (DTI), 792–793, 793f
overview, 789
Mammalian embryo culture medium (recipe), 115
Mammalian embryo dissection medium (recipe), 115
Mammalian forebrain, time-lapse imaging of fluorescently labeled live cells in embryonic, 341–355
imaging setup, 342–343
basic setup, 342–343
objective choice, 343
labeling cells, 341–342
overview, 341–342
protocol, 344–354
assembling images into a time-lapse sequence, 351–352, 352f
brain dissection dishes, preparation of, 345

Mammalian forebrain, time-lapse imaging of fluorescently labeled live cells in embryonic (*Continued*)
brain removal and embedding, 347–348
data acquisition and processing, 350–351, 350f
embryo removal, 346, 347f
experimental method, 345–352
material, 344–345
plating slices in culture wells, 348–350, 349f
preparation for surgery and sectioning, 345–346
recipes, 354
troubleshooting, 352–353
vibratome sectioning, 348
Mammary organoids, isolation for long-term time-lapse imaging (protocol), 640–643
Mantle cells, of lateral-line system, 271
MARCAM (mosaic analysis with a repressible cell marker), 3
dual-expression-control, 160
examples of applications, 158f, 162–164
analysis of neuronal morphogenesis, 163–164, 164f
live imaging, 163
tracing neural circuits, 162–163
MADM (mosaic analysis with double markers) compared to, 161–162
principle of, 159–160, 160f
protocol in *Drosophila*, 166–168
experimental method, 166–167
imaging setup, 166
materials, 166
troubleshooting, 167–168
Q system–based, 160
twin-spot, 160
Marking cells for imaging morphogenetic behavior and cell fates in mouse embryos, 311–318
general instructions for cell marking experiments, 315
imaging setup, 312, 313
overview, 311–312
protocols
electroporation of mouse embryos, 323–326
experimental method, 324f, 325–326
materials, 323, 325
troubleshooting, 326
grafting cells into mouse embryo, 320–322
experimental method, 321–322, 322f
materials, 320
troubleshooting, 322
painting mouse embryos, 317–319
experimental method, 318–319
materials, 317–318
troubleshooting, 319
preparation and in vitro culture of mouse embryos, 314–315
experimental method, 314–315
materials, 314
preparation of micropipettes, 316
recipes, 328
MATLAB (The MathWorks), 501, 505, 528, 595
Matrigel (BD Biosciences), 606, 638, 640, 642
M9 buffer (recipe), 20, 243
mCherry
axon labeling, 438–439, 438f
dynamic imaging of developing vasculature, 660, 661f
fluorescent transgene expression in mouse embryos, 103f, 104
in Fucci probe derivatives, 332
imaging axonal transport, 461, 462f
in live imaging of *C. elegans,* 13
in live imaging of *Xenopus,* 401, 401f
Mean squared displacement (MSD), 546
Melanophores, zebrafish, 50
MEMFA (recipe), 736
Mercury arc lamp, 833, 834
MESAB (30x) (recipe), 197, 251
Metamorphosis, in *Drosophila,* 26
Metamorph software (Molecular Devices, Inc.), 13, 364, 420
Metanephric mesenchyme. *See* Kidney development, imaging
Methanol, for dehydration of mouse embryo, 749–750
Methylcellulose, 20, 258
Methylene blue, 273, 284
Methylene chloride, for dissolving carbocyanine dyes, 179
Microinjection
in *Xenopus*
targeted microinjection on mRNA encoding fluorescent proteins, 73, 74f
in zebrafish, 51
constructing a microinjection chamber for eggs, 56
DNA injection into early embryos, 411–412
DNA injection to generate transiently transgenic retinal progenitor cells, 260
Kaede mRNA for cell fate studies, 276–278
mRNA microinjection for notochord formation study, 570, 572–573
protocol, 53–55, 54f
μManager software, 235–238, 452
Micropipettes, preparation of
holding pipettes, 316
injection pipettes, 316
Microscope objective lens, 835–836
Microscopic magnetic resonance imaging (μMRI)
developmental atlas, 793–797
labeling anatomy, 794–795, 796f
mouse, 794
quail, 794, 795f
visualizing developing anatomy from atlases, 796–797
live imaging
amphibian development, 791–792, 791f
avian cardiac development, 792
diffusion tensor imaging (DTI), 792–793, 793f
as nondestructive imaging, 740
overview, 789
Microtome, 768, 770, 775
Microtubule-based vesicle transport, 461–462, 462f
Micro-ultrasound imaging
as nondestructive imaging, 741
as noninvasive imaging, 741
of normal ocular development
ocular microcirculation, 677, 677f
primary ocular tissues, 676, 676f
ocular disease models, 678–679
glaucoma, 678–679, 679f
retinoblastoma, 678, 678f
procedures for imaging of mice (protocol), 673–675
resolution, wavelength, and maximum imaging depth versus frequency, 672, 672t
technology overview, 670, 671f, 672, 672t
MicroXCT, 754, 755
Minimal medium (recipe), 369
mKate, 251
m-Message m-Machine kit, 276
Model system
atlases for, 7–8
overview, 2
Modified Barth's saline (MBS) (recipe), 385
Modified Barth's solution (MBS) (1x) (recipe), 566
Modified ringer's solution (recipe), 369
MORE-Cre transgenic line, 301
Morphogenesis
cellular basis of, 7
live imaging in *Drosophila*, 29
live imaging in zebrafish, 50–51
long-term imaging of epithelial morphogenesis on three-dimensional organotypic cultures, 623–645
bringing sample to microscope stage (practical), 631–633, 633f
bringing sample to microscope stage (theory), 629–631
environmental control, 633–639, 634f
isolation of mouse mammary organoids for long-term time-lapse imaging (protocol), 640–643
limiting phototoxicity and photobleaching, 628–629
microscopic requirement issues, 626–628
overview, 623–625
temperature issues, 633–637
molecular mechanisms and cellular mechanics of in *Xenopus,* 551–567
overview, 551–552
protocols
assembly of chambers for stable long-term imaging of live tissue, 558–559
imaging processing and analysis, 563–566
imaging strategies for collecting long-term time-lapse sequences with minimal photodamage, 560–562
microsurgical approaches to isolate cells and tissues: explant preparation, 555–557
recipes, 566
sample preparation for using live reporters, 553–554
notochord formation in zebrafish, 569–579
Morphogen gradient, 29
applications of quantitative measurements and kinetics, 534

bicoid, 523–532
equipment and software for quantitative imaging of, 534t
measuring kinetic parameters of morphogen spreading using FRAP, 538–542, 539f
bleaching depth and photodamage, 540
choice of region of interest, 540–541
detection sensitivity, 541
intracellular and extracellular pools, 542
photobleaching during image acquisition, 541
theoretical analysis of FRAP experiments, 541–542
tissue geometry and subcellular morphogen distribution, 539–540
measuring shape of, 534–538, 535f
calibrating fluorescence intensity to molecular number, 537
imaging in linear range of detection, 536–537
quantifying gradient shape, 537–538
measuring subcellular morphogen dynamics using particle tracking, 542–547
parameters of endosomal dynamics, 546–547
particle detection, 543, 544f, 545
particle tracking, 544f, 545–546
quantitative measurements in *Drosophila* imaginal discs, 533–550
overview, 533–534
Morphogens, 6, 533
Morpholinos, electroporation of
in chick embryos, 120
single-cell electroporation (SCE) in *Xenopus,* 148
Mosaic analysis with a repressible cell marker. *See* MARCAM (mosaic analysis with a repressible cell marker)
Mosaic analysis with double markers. *See* MADM (mosaic analysis with double markers)
Mosaic embryos
generating *Xenopus* for imaging and analysis, 75–76, 75f
making zebrafish mosaic primordia by focal electroporation, 279–281, 280f
Mosaic labeling, of zebrafish retinal cells
DNA injection to generate transiently transgenic retinal progenitor cells, 260
transplantation of transgenic progenitor retinal cells expressing fluorescent markers, 256–259
Mounting
in agarose, 262, 274, 422, 428
C. elegans embryos, 15–20, 16f
agar mounts, 231–234, 232f, 233f
Drosophila embryo in DePex, 704
Drosophila tissues
general considerations, 33–34
protocol, 35–36
mouse embryo, 750, 750f
mouse retina explant, 422
Xenopus embryos, 376–378, 377f
zebrafish embryos, 274, 382, 383f
for notochord formation study, 574–575
for retinal development imaging, 261–262, 262f, 427–428
for synaptogenesis imaging, 412, 413f
Mouse
cannibalism, minimizing, 514
developmental atlas, 794, 795, 796f
isolation of mouse mammary organoids for long-term time-lapse imaging (protocol), 640–643
kidney development, 605–621
MADM (mosaic analysis with double markers) protocol, 169–173
micro-ultrasound imaging of eye development, 669–681
neuromuscular junction, imaging, 435–448
in vitro imaging of retinal whole mounts, 419–425
discussion, 424
examples, 424, 425f
experimental method, 421–423
image acquisition, 422–423
imaging setup, 419–420
labeling, 422
materials, 420–421, 421f
mounting, 422
retinal explant preparation, 421–422
troubleshooting, 423–424
Mouse brain
cranial window surgery, 514, 516–517
genetic labeling of neurons, 199–216
achieving robust and specific neuron labeling, 204–206
Cre/loxP system, 204
driver alleles, technical tips on, 206
transcription activation system, 204
transgenic overexpression, 206
viruses as reporter components in binary systems, 205–206, 205f
binary expression systems, gene targeting and, 202–203, 202f, 203f
Cre-dependent adeno-associated virus preparation and delivery (protocol), 209–213
AAV delivery, 211–212
AAV production and serotypes, 211
imaging setup, 209
materials, 209–210
troubleshooting, 212–213
viral vector design, 210–211
overview, 199
relative merits of methods, 208
binary system versus direct labeling, 208
expression levels, 208
gene targeting versus transgenesis, 208
specificity and reliability of cell labeling, 200–202
gene targeting approach, 201f, 202
transgenic approach, 200–202, 201f
strategies
Brainbow, 207
intersectional recombination, specificity increase through, 206–207, 207f
mosaic analysis with double markers, 207
single-neuron labeling with inducible Cre-mediated knockout (SLICK), 207
in vivo imaging of axonal and dendritic structures in developing cortex, 513–522
overview, 513–514
protocol, 515–521
Mouse embryos
cardiovascular development, imaging, 659–668
confocal microscopy of vital fluorescent proteins, 660–663, 664f
dynamic imaging of developing vasculature, 660–662, 661f
hemodynamic analysis with fast-scanning confocal microscopy, 662–663, 664f
optical coherence tomography (OCT) imaging, 664–667, 665f
Doppler imaging of blood flow, 666–667
experimental system, 664–666
live structural imaging, 666
overview, 659–660
cell movement imaging in egg cylinder stage embryos, 299–309
overview, 299–301
protocol, 302–309
experimental method, 303–307
imaging setup, 302
materials, 302–303
recipes, 309
troubleshooting, 307–308
dissection of, 109–110, 110f
electroporation, 119–142
advantages and disadvantages of, 327
of endoderm, 325
of gastrula-stage germ layers, 326
of mesoderm or ectoderm, 325–326
overview, 119–121
protocols
analysis of development following electroporation, 137
assembly of electrodes and wiring, 122–123, 122f
electroporation method, 136
marking cells for imaging morphogenetic behavior and cell fates, 323–326
preparation of culture medium, 133–134
preparation of embryos, 135
troubleshooting, 138
staging and electroporation parameters, 134t
in utero, 138
harvesting, 314
large-field high-resolution observation of tissue sections from Fucci mouse embryos, 337–339
live imaging, 101–117
advantages and limitations of, 114–115
examples, 104
cell behavior and endoderm morphogenesis in gastrula, 104
vascular development and cardiac function, 104
fluorescent transgene expression in, 103f
imaging early development, 102–103, 103f
immobilization of embryos, 110–111, 114
protocols

Mouse embryos (*Continued*)
preparation of postimplantation mouse embryos, 109–111, 110f
preparation of rat serum for culturing mouse embryos, 107–108, 108f
time-lapse imaging of postimplantation mouse embryos, 112–113
recipes, 115
setup, 105, 105f, 106f
magnetic resonance imaging (MRI), high-throughput analysis by, 777–787
overview, 777–778
protocol, 779–787
data reconstruction and analysis, 782–785, 783f, 784f
discussion, 786
embryo preparation, 780–782
experimental method, 780–785
imaging setup, 779
materials, 779–780
recipes, 786–787
troubleshooting, 785
optical projection tomography (OPT), 739–752
apparatus for obtaining images, 742f
how it works, 741–743, 742f
imaging modes, 742
labeling issues, 744–746
histology/anatomy of unstained specimens, 745
immunohistochemistry, 745–746
lipophilic dyes for tracing axons and cell movements, 746
reconstruction artifacts in overstained specimens, 745f
in situ hybridization, 746
transgenic reporter constructs, 746
preparation of mouse embryos for imaging (protocol), 747–750
experimental method, 747–750
materials, 747
recipes, 751
overview of development, 101–102
Mouse Genome Database, 648
Mouse Genome Informatics (website), 609, 648
Mouse serum, preparation of, 303–304
MRI. *See* Magnetic resonance imaging (MRI)
mRNA
localization studies in *Drosophila*, 28
synthesis of MRNA encoded fluorescent proteins, 553
mRNA microinjection
in *Xenopus*
targeted microinjection on mRNA encoding fluorescent proteins, 73, 74f
in zebrafish
Kaede mRNA for cell fate studies, 276–278, 277f
notochord formation study, 570, 572–573
Multicolor Brainbow imaging. *See* Brainbow
Multiphoton microscopy
high-resolution, multiphoton time-lapse imaging of early chick embryos, 581–592
live imaging in zebrafish, 52
as nondestructive imaging, 740–741
Murray's clear, 733, 741
mVenus, in Fucci probe derivatives, 332
myr-Venus, 608

N

nacre mutant, zebrafish, 50
National Center for Biomedical Ontology, 795
N-cadherin, 406, 407f
Nectins, 406
Neural crest cell migration
in chick explant cultures, 296f, 297
live imaging in chick embryos, 90–91
Neurexins, 406
Neuroblast lineage imaging within intact larval brains in *Drosophila,* 217–227
overview, 217–219
example studies, 218–219, 218f
fusion lines, 218t
neuroblast Gal4 driver lines, 219t
protocol, 220–224
image acquisition, 223
imaging setup, 220, 221f
larval dissection, 221–222
materials, 220–221
recipes, 225
specimen orientation and slide sealing, 222
troubleshooting, 223–224
Neurogliaform cells (NGFCs), genetic labeling of, 206
Neuromasts, of lateral-line system, 271–272
Neuromuscular junction, imaging mammalian, 435–448
overview, 435–441
axon labeling, 436–437
distinguishing one input from another, 438–439, 438f, 440f
photoxicity, 440–441
in vivo imaging, 437–438
in vivo imaging controls, 439–440
in vivo optical access to tissue, 436, 436f
protocol, 442–447
anesthesia, 443–444
discussion, 447
experimental method, 443–445
imaging, 445
imaging setup, 442
intubation, 444
materials, 442–443
recovery, 445
surgery, 444
troubleshooting, 445–446
Neuronal circuit
imaging, 6
tracing with MARCAM, 162–163
Neuronal morphogenesis, MARCAM analysis of, 163–164
Neuronal transfection, by single-cell electroporation (SCE) in *Xenopus,* 146–147, 149–153
Neurons
genetic labeling in mouse brain, 199–216
hippocampal neurons in culture, imaging, 449–465
number in human brain, 157
simultaneous imaging of structural plasticity and calcium dynamics in developing dendrites and axons, 479–489
simultaneous patch-clamping and calcium imaging in developing dendrites, 491–498
single-neuron labeling using genetic methods, 157–175
synaptic protein dynamics, imaging, 499–512
time-lapse imaging of neuronal development in *Xenopus,* 387–404
Neutral-density filter, 830
NgCAM, 461, 462f
NGFCs (neurogliaform cells), genetic labeling of, 206
NIH Image analysis software, 391
N-methyl-D-aspartate receptors (NMDARs), 164
NmuMG/Fucci2 cell line, 332, 333–336
Nodal$^{lacZ/\Delta 600}$ mouse mutant, 299
Noise
signal-to-noise ratio, MRI, 790
sources of measurement, 530
Nondestructive imaging, 740–741
confocal microscopy and multiphoton microscopy, 740–741
microscopic magnetic resonance imaging (μMRI), 740
microscopic ultrasound imaging, 741
optical coherence tomography (OCT), 741
X-ray micro-computed tomography (μCT), 740
Notochord formation in zebrafish, 569–579
blastomere injection of cleavage-stage embryos and imaging of labeled cells (protocol), 571–578
discussion, 577
experimental method, 572–576
imaging, 575–576
imaging setup, 571
labeling embryos, 572–573
materials, 571–572
mounting, 574–575
recipes, 578
troubleshooting, 576–577
cell labeling techniques, 570
overview, 569–570
NP-EGTA-AM, 367, 368
N-phenylthiourea (PTU), 50
Nuclear mask, 690
Nucleofection, 454, 456

O

Object-Image software, 391, 392f
Objective lens, 835–836
heater, 635–636
high-NA oil-immersion lens, 561
water-immersion lens, 561, 632
Observation medium (recipe), 385
OCT. *See* Optical coherence tomography (OCT) imaging
Octadecyl (C18) indocarbocyanines (DiI and DiD), 178–179
Oct4 promoter, 103
Olfactory receptor neuron, tracing circuit with MARCAM, 162–163
Ontologies, 795
Open Biomedical Ontologies Foundry, 795
OPT. *See* Optical projection tomography (OPT)
Optical coherence tomography (OCT) imaging, 7
of beating avian heart, 647–655
imaging early quail heart (protocol), 655
methods and results, 650–654, 651f–654f

overview, 649–650
of cardiovascular development in mouse embryo, 664–667, 665f
Doppler imaging of blood flow, 666–667
experimental system, 664–666
live structural imaging, 666
four-dimensional (4D), 650–655
frequency domain (FD-OCT), 650
as nondestructive imaging, 741
swept-source (SS-OCT), 651–652, 654f, 655
time-domain (TD-OCT), 651–652
Optical drift, temperature effect on, 634
Optical equipment, cleaning, 835–836
Optical projection tomography (OPT), 739–752
apparatus for obtaining images, 742f
applications in developmental biology, 743–744
analyzing gene expression patterns at mRNA or protein level, 743–744
anatomical atlases, 743
distribution of labeled subpopulations of cells, 744, 744f
phenotyping, 743
future prospects, 751
how it works, 741–743, 742f
imaging modes, 742
emission tomography (fluorescence OPT), 742
transmission imaging (bright-field OPT), 742
labeling issues, 744–746
histology/anatomy of unstained specimens, 745
immunohistochemistry, 745–746
lipophilic dyes for tracing axons and cell movements, 746
reconstruction artifacts in overstained specimens, 745f
in situ hybridization, 746
transgenic reporter constructs, 746
preparation of mouse embryos for imaging (protocol), 747–750
experimental method, 747–750
dehydration, clearing, and mounting, 749–750, 750f
embedding, 748, 749f
fixing, 747
trimming, 748–749
materials, 747
recipes, 751
Oregon Green, 187
Oregon Green BAPTA, 388, 482–484, 493–494, 494f
Organogenesis, in *Drosophila* embryos, 26
Organoid medium (branching) (recipe), 643
Organoid medium (simple) (recipe), 643
Organotypic culture
live imaging of *Xenopus* embryo explant, 82
long-term imaging of epithelial morphogenesis on three-dimensional organotypic cultures, 623–645
bringing sample to microscope stage (practical), 631–633, 633f
bringing sample to microscope stage (theory), 629–631
environmental control, 633–639, 634f
isolation of mouse mammary organoids for long-term time-lapse imaging (protocol), 640–643
limiting phototoxicity and photobleaching, 628–629
microscopic requirement issues, 626–628
overview, 623–625
temperature issues, 633–637
preparation of organotypic hippocampal slice cultures, 502–505
brain dissection, 504
experimental method, 503–505
feeding slices, 505
hippocampal dissection and slicing, 504
materials, 502
plate preparation, 503, 503f
plating slices, 504
sterile hood setup, 503–504
simultaneous imaging of structural plasticity and calcium dynamics in developing dendrites and axons, 479–489
synaptic protein dynamics, imaging, 499–512
Otx2 mouse mutant, 299
Oxacarbocyanine (DiO), 178–179

P

PA-GFP. *See* Photoactivatable green fluorescent protein (PA-GFP)
Painting mouse embryos
advantages and disadvantages of, 327
for imaging morphogenetic behavior and cell fates, 317–319
Pal-1 RNA interference, 230
Paraformaldehyde, for mouse embryo fixation, 113
Patent ductus arteriosus, 647
Pax8/rtTA strain, 608
PB1 medium (recipe), 328
PBS. *See* Phosphate-buffered saline (PBS) (recipe)
PBS with Triton X-100 (recipe), 751
Pcsk5, 786
P element, 32–33
Peltier device, 14
Perfusion chamber, for retinal explants, 420–421, 421f
Phallusia mammillata, time-lapse imaging of, 713–715
Phenotyping, 8, 743
Phenylthiourea (PTU), 50
PhiC31 system, 32, 33
Phosphate-buffered saline (PBS) (recipe), 288, 566, 728, 736, 751, 786–787, 824
Phosphotungstic acid, 755, 763
Photoactivatable green fluorescent protein (PA-GFP)
in imaging synaptic protein dynamics, 500, 506–509, 508f
in *Xenopus,* 401–402, 401f
Photoactivation cell labeling
of chick embryos, 87f, 89, 92
in *Drosophila*, 29
Photobleaching
FRAP (fluorescent recovery after photobleaching), 541
of green fluorescent protein (GFP), 530
limiting in long-term time-lapse movies, 628–629
Photoconvertable protein
Kaede use in birthdating in zebrafish, 245–250, 246f, 247f
Kaede use in labeling defined cells in zebrafish embryos, 276–278, 277f
KikGR and cell movement imaging in egg cylinder stage mouse embryos, 300f, 301
Photodamage
FRAP (fluorescent recovery after photobleaching), 540
imaging strategies for collecting long-term time-lapse sequences with minimal, 560–562, 561f
Photon energy, 827
Phototoxicity
in fluorescent imaging
in live imaging of *C. elegans,* 13
in neuromuscular junction imaging, 440–441
limiting in long-term time-lapse movies, 628–629
in time-lapse experiments, 595
Physical sectioning techniques, 739–780. *See also specific applications*
Piccolo, 406
Pinch1, 786
Plasmid DNA. *See also* DNA
electroporation of mouse embryos (protocol), 323–326
endotoxin-free, 147
preparation for electroporation, 121
Point clouds
conversion of images to, 704–706, 705f
registration into a virtual embryo, 706, 707f
PointCloudXplore visualization tool, 706–707, 708f
Polyvinylpyrrolidone (PVP), coating tubing with, 178
Preparation medium, GBSS (recipe), 488
Projecting images, 564–565, 564f
Promoter, tissue-specific, 32
Pronase, 258
Proneuromasts, 272
Proportional integral derivative (PID) controller, 636, 637
ProStack software, 689
Protein trap, in *Jupiter* gene, 225
Protocadherin-α, 406
Protocadherin-1γ, 407f
PSD95, 424, 425f
PTA stain (recipe), 763
Ptdsr, 786
PTU stock (50×) (recipe), 64, 432
PTU water (recipe), 197, 251
PVP (polyvinylpyrrolidone), coating tubing with, 178

Q

Q system, in MARCAM (mosaic analysis with a repressible cell marker), 160
Quail
developmental atlas, 794, 795f
magnetic resonance imaging (MRI), 794, 795f
optical coherence tomography (OCT) imaging of early heart, 651–655, 651f–654f
quail-chick chimera, 582

Quail development, four-dimensional fluorescent imaging of, 593–604
4D fluorescent imaging of quail embryos (protocol), 597–604
experimental method, 598–602
image analysis, 601–602, 601f–602f
inverted imaging of in vitro embryos, 599
multitime macro imaging, 599
paper ring preparation, 598
sample setup for in vitro imaging, 598–599, 598f
tiled *z*-stack time-lapse experiments, 599–600, 600f
imaging setup, 597
materials, 597–598
recipe, 604
troubleshooting, 602–603
overview, 593–595
image analysis, 594–595
microscopy equipment requirements, 594
in vitro culturing, 594
pre-imaging considerations, 595–596
data storage hardware, 596
data volumes in multidimensional imaging, 596t
environmental control, 595
fluorophore compatibility, 595
magnification, 595
Quantitative imaging of gene expression in *Drosophila melanogaster,* 683–697
confocal microscopy, 689
image and data processing methods, 689–695
background removal, 691–693, 692f
data averaging, 694–695, 695f
image registration, 694
image segmentation, 689–691
temporal characterization of embryos, 693–694
method overview, 684, 685f
overview, 683–684
preparation of embryos (protocol), 686–688
embryo collection and fixation, 687
immunostaining, 687–688
materials, 686–687
troubleshooting, 688
recipes, 696
QUASAR (quiet spectral array) detector, 439

R

Rab3, 406
Rac GTPases, 163
Ramón y Cajal, Santiago, 157, 159
Rat serum for culturing mouse embryos, 107–108, 108f
RCE reporter, 204
Reagents, for live imaging in *Drosophila melanogaster,* 837t–838t
Recipes
aCSF solution (1x), 354
aCSF stock solution A, 354
aCSF stock solution B, 354
agarose (0.5% w/v), 763
albumin-agarose, 604
Ames medium, 432
anesthetic medium, 384
apple (or grape) juice agar, 696
apple juice agar plates, 43
artificial cerebrospinal fluid (aCSF), 432, 432t, 510
artificial cerebrospinal fluid (aCSF) stock solutions, 354
artificial seawater-HEPES (ASWH), 727
bathing saline solution, 476
Boyd buffer, 20
calcium blocker cocktail, 369
calcium-free saline, 369
calcium phosphate transfection buffer, 476
collagenase solution, 643
culture medium, 488, 618
Danieau's medium (30x), 432, 432t
Danilchik's for Amy (DFA) medium, 566
depolarizing buffer, 476
dissection medium, 510
divalent-cation-free medium, 369
DNA solution for injection, 64
DR75, 328
for *Drosophila melanogaster*, 838–839
HL3 solution, 838
supplemented D-22 insect medium, 838
supplemented Schneider's medium 1, 838
supplemented Schneider's medium 2, 839
supplemented Shields and Sang M3 insect medium 1, 839
supplemented Shields and Sang M3 insect medium 2, 839
supplemented Shields and Sang M3 insect medium 3, 839
zero-calcium HL3 solution, 839
E3 buffer, 414
E3 embryo medium (60x), 385
embedding agarose, 415
embryo embedding agar, 385
embryo embedding agarose, 267
embryo glue, 43
embryo medium, 64, 578
embryo medium (E3M) (60x stock solution), 268
embryo time-lapse solution, 268
E3 medium (60x stock), 824
external solution, 497
fixation buffer, 696
fixative solution, 476
fix solution, 728
Fluo-3AM or Fluo-4AM, 369
4F1G, 763
Holtfreter buffer, 268
internal solution, 497
kynurenic acid stock solution (100 mM), 488
low-melting-point agarose, 432
mammalian embryo culture medium, 115
mammalian embryo dissection medium, 115
M9 buffer, 20, 243
MEMFA, 736
MESAB (30x), 197, 251
minimal medium, 369
modified Barth's saline (MBS), 385
modified Barth's solution (MBS) (1x), 566
modified ringer's solution, 369
observation medium, 385
organoid medium (branching), 643
organoid medium (simple), 643
PB1 medium, 328
PBS with Triton X-100, 751
phosphate-buffered saline (PBS), 288, 566, 728, 736, 751, 786–787, 824
preparation medium, GBSS, 488
PTA stain, 763
PTU (50x), 64, 432
PTU water, 197, 251
recording solution, modified HBSS, 488
Ringer's solution, 298
RNA solution for injection, 65
slice culture medium, 354, 511
spike induction saline, 370
SSC (20x stock solution), 736
Steinberg's solution, 403
supplemented CMRL medium, 309
tadpole rearing solution, 154
TBS, 736
tricaine (20x), 64–65, 433
Trolox, 489
tyrode Ringer's saline, Ca^{2+}/Mg^{++}-free, 328
Valap, 243
Recording solution, modified HBSS (recipe), 488
Red fluorescent protein (RFP)
fluorescent transgene expression in mouse embryos, 103f, 104
retinal development imaging in zebrafish, 254, 256, 260
use in zebrafish, 51
Reichert's membrane, removal of, 305f, 306
Ret-GFP mice, 608
Retinal circuits, imaging of, 417–434
general imaging considerations, 418
overview, 417–418
protocols, 419–433
in vitro imaging of retinal whole mounts, 419–425
discussion, 424
examples, 424, 425f
experimental method, 421–423
image acquisition, 422–423
imaging setup, 419–420
labeling, 422
materials, 420–421, 421f
mounting, 422
retinal explant preparation, 421–422
troubleshooting, 423–424
in vivo imaging of zebrafish retina, 416–431
discussion, 430, 430t, 431f
examples, 430, 431f
experimental method, 427–428
image acquisition, 428
imaging setup, 426
materials, 426–427, 427f
mounting embryos, 427–428
transgenic lines expressing in retina, 430t
troubleshooting, 428–429
Retinal ganglion cell (RGC)
bulk electroporation in live *Xenopus* tadpoles, 399–402
dye labeling axons in live *Xenopus* tadpoles, 396–398, 398f
electroporation in *Xenopus,* 389
Retinal neurons, ballistic labeling of developing, 177–190
Retinal progenitor lineages in developing zebrafish retina, imaging, 253–268
imaging setup, 254–255
acquisition, 254
processing, 255
overview, 253–254, 267

protocols
DNA injection to generate transiently transgenic retinal progenitor cells, 260
embedding embryos, imaging, staining, and image processing of developing zebrafish retina, 261–267
experimental method, 261–265
materials, 261
troubleshooting, 265–266
recipes, 267–268
transplantation of transgenic progenitor retinal cells expressing fluorescent markers, 256–259
dechorionation of embryos, 257–258
experimental method, 257–259
materials, 256–257
Retinoblastoma, 675
Reverse tetracycline transactivator (rtTA), 608
RFP. *See* Red fluorescent protein (RFP)
Rho GTPases, 163
Ringer's solution (recipe), 298
RNAi, in *Drosophila,* 33
RNA microinjection in zebrafish, 51
constructing a microinjection chamber for eggs, 56
protocol, 53–55, 54f
RNA solution for injection (recipe), 65
ROI Manager, 565
Rosa26, use in genetic labeling of neurons in mouse brain, 204
ROSA26-MADM, 169–171
Rosa26R reporter transgene, 327
Roy orbison mutant, zebrafish, 50, 430
R26R-eYFP reporter, 300f, 301

S

Sagittal slice explant culture, chick, 291–298
Sall1-GFP, 608
ScanImage, 501, 515
SCF^{Skp2} complex, 332
Sectioning techniques, 739–780. *See also specific applications*
Self-cleaving peptide T2A, 206
Septal defects, 647–648
Shields and Sang M3 insect medium, 38
Short hairpin RNA (shRNA), electroporation of in chick embryos, 120
single-cell electroporation (SCE) in *Xenopus,* 148
Signal-to-noise ratio, MRI, 790
Silicon intensified target (SIT) video camera, 437, 447
Single-cell electroporation (SCE), of rat hippocampal neurons, 483f, 484
Single-cell electroporation (SCE) in *Xenopus,* 143–155
efficiency, factors influencing, 144–146
electrical stimulus parameters, 145
glass micropipettes, 144–145
microscopy, 146
electroporation of tadpole tectal neurons (protocol), 149–154
expected results, 152
limitations, 153
materials, 149–150
method, 150–151
recipes, 155
special considerations, 153
troubleshooting, 152
implementation, 146–148
coelectroporation of fluorescent dye space fillers with morpholinos or peptides, 148
of DNA for neuronal transfection, 146–147, 147f
fluorescent dyes, 147–148
with tadpole optic tectum, 146
labeling individual neurons in the brains of live tadpoles by electroporation of dyes or DNA (protocol), 393–395
overview, 143, 144
setup, 145f
Single-neuron labeling using genetic methods, 157–175
advantages and limitations, 164–165
comparing genetic methods with Golgi staining, 164–165
relative merits of different genetic methods, 165
examples of applications, 158f, 162–164
analysis of neuronal morphogenesis, 163–164, 164f
live imaging, 163
tracing neural circuits, 162–163
genetic labeling of neurons in mouse brain, 207
MADM (mosaic analysis with double markers)
principle of, 160–162, 161f
protocol in mice, 169–173
MARCAM (mosaic analysis with a repressible cell marker)
principle of, 159–160, 160f
protocol in *Drosophila,* 166–168
overview, 157–158
protocols, 166–173
MADM (mosaic analysis with double markers) in mice, 169–173
MARCAM (mosaic analysis with a repressible cell marker) in *Drosophila,* 166–168
single-neuron labeling with inducible Cre-mediated knockout (SLICK), 207
uses of, 158–159
Single-neuron labeling with inducible Cre-mediated knockout (SLICK), 207
Site-specific integration, 32
Site-specific *trans*-recombination. *See* MADM (mosaic analysis with double markers); MARCAM (mosaic analysis with a repressible cell marker)
Six2 gene, 608
SkyScan 1174, 754
Slice culture medium (recipe), 354, 511
Slice cultures, time-lapse imaging of fluorescently labeled live cells in embryonic mammalian forebrain, 341–355
imaging setup, 342–343
labeling cells, 341–342
overview, 341–342
protocol, 344–354
Slice explant culture, chick, 291–298
SLICK method, 165, 172
SNAP-25, 406
SNLauncher software, 803, 805, 805f
Sox4, 786
Spatiotemporal dynamics of multicellular cell-cycle progressions, 331–340
Spike induction saline (recipe), 370
Spinal neurons, imaging calcium transients in *Xenopus,* 357–371
advantages and limitations, 358
imaging setup, 358
overview, 357–358
protocols
imaging and analysis of *Xenopus* spinal neurons, 361–364
perturbation of calcium dynamics in *Xenopus* spinal neurons, 365–368
preparation of *Xenopus* neuronal tissues for imaging, 359–360
recipes, 369–370
Sprat, N.T., 582
SSC (20× stock solution) (recipe), 736
Stage-top incubator, 637
StarryNite software, 803, 804–805, 811–812
Steinberg's solution (recipe), 403
Stimulated emission depletion (STED) microscope, 632
Superresolution, 545
Supplemented CMRL medium (recipe), 309
Supplemented D-22 insect medium (recipe), 838
Supplemented Schneider's medium 1 (recipe), 838
Supplemented Schneider's medium 2 (recipe), 839
Supplemented Shields and Sang M3 insect medium 1 (recipe), 839
Supplemented Shields and Sang M3 insect medium 2 (recipe), 839
Supplemented Shields and Sang M3 insect medium 3 (recipe), 839
Surface Evolver, 718
SV2, 406, 407
Sylgard, 344–345
Synapins, 406
Synapse formation and function in neuronal cell cultures, 467–477
fluorescent protein fusions useful as markers of synaptic components, 470t
imaging by quantitative immunocytochemistry (protocol), 468–476
discussion, 475
experimental method, 469–474
assay of synaptic function at single synapse level, 471–472
image analysis, 472–474, 473f, 474f
immunostaining and image acquisition, 472
neuronal cell culture, 469
transfection, 469–471
imaging setup, 468
materials, 468–469
recipes, 476
troubleshooting, 474–475
overview, 467
Synaptic protein dynamics, imaging, 499–512
imaging setup, 500–501, 501f
overview, 499–501
preparation of organotypic hippocampal slice cultures, 502–505
brain dissection, 504

Synaptic protein dynamics, imaging (*Continued*)
experimental method, 503–505
feeding slices, 505
hippocampal dissection and slicing, 504
materials, 502
plate preparation, 503, 503f
plating slices, 504
sterile hood setup, 503–504
protocols, 502–511
imaging synaptic protein dynamics using photoactivatable GFP, 506–510
analysis, 509
choosing photoactivation and imaging wavelengths, 507
discussion, 510
experimental method, 506–509
materials, 506
neuronal transfection, 506–507
photoactivation, 507–508, 508f
preparation of PA-GFP-tagged proteins, 506
time-lapse imaging of fluorescence decay, 508–509
recipes, 510–511
in vitro versus in vivo preparation, 500
Synaptogenesis, imaging in zebrafish, 405–415
advantages and limitations, 414
fluorescence imaging of transgenic embryos (protocol), 410–415
discussion, 414
experimental method, 411–413
imaging setup, 410
injection of DNA, 411–411
materials, 410–411
mounting embryos, 412, 413f
recipes, 414–415
time-lapse data collection, 412–413
fluorescent tagging of synaptic proteins, 406–409, 407f, 408f
bacterial artificial chromosomes (BACs), 408–409, 408f
Gal4-UAS system, 407–408
promoters/enhancers, 407–409
overview, 405–409
coexpression of transgenes, 409, 409f
fluorescent tagging of synaptic proteins, 406–409, 407f, 408f
synaptic puncta, identification of, 414
Synaptophysin, 406, 407f
SynCam, 406
Syntaxin-1, 406
Syt-1, 473, 473f, 474f
SYTOX Green, 704

T

T2A (self-cleaving peptide), 206
Tadpole rearing solution (recipe), 154
Tamoxifen, 169
TBS (recipe), 736
Td-Tomato
cell movement imaging in egg cylinder stage mouse embryos, 300f, 301
retinal ganglion cell (RGC) labeling, 424, 425f
Teflon membrane, 86f, 88, 94, 95f
Temperature issues in long-term imaging on organotypic cultures, 633–637
TetO reporter, 203, 204
Tetracycline-inducible expression, 92
Tetracycline trans-activator (tTA), 203, 204
Tetralogy of Fallot, 647
Thapsigargin, 366
Three-dimensional embryo replicas, creating, 711–728
overview, 711–712
protocols
imaging of fixed *Ciona* embryos, 716–717
recipes, 727–728
reconstruction, 718–726
Arima segmentation, 720–723, 721f–723f
data pretreatment, 719–720, 719f
experimental method, 718–726
file format, 718–719
history of files used, 726t
imaging setup, 718
object editing, 724–726
troubleshooting, 726
time-lapse imaging of live *Phallusia* embryos, 713–715
reconstruction flowchart, 712
Three-dimensional morphology of *Drosophila* blastoderm, 699–710
3D Virtual Embryo software, 712, 723f, 727
Thy1 promoter, 194, 206, 436–437, 447
Tie2 promoter, 104
Time-lapse imaging
cardiovascular development in mouse embryos, 660–663, 664f
dynamic imaging of developing vasculature, 660–662, 661f
hemodynamic analysis with fast-scanning confocal microscopy, 662–663, 664f
cell labeling techniques, 570
cell movements in egg cylinder stage mouse embryos, 307
fluorescently labeled live cells in embryonic mammalian forebrain, 341–355
imaging setup, 342–343
basic setup, 342–343
objective choice, 343
labeling cells, 341–342
overview, 341–342
protocol, 344–354
assembling images into a time-lapse sequence, 351–352, 352f
brain dissection dishes, preparation of, 345
brain removal and embedding, 347–348
data acquisition and processing, 350–351, 350f
embryo removal, 346, 347f
experimental method, 345–352
material, 344–345
plating slices in culture wells, 348–350, 349f
preparation for surgery and sectioning, 345–346
recipes, 354
troubleshooting, 352–353
vibratome sectioning, 348
hippocampal neurons in culture, 455–459
image processing and analysis
kymographs, 563, 563f
managing your region of interest, 565
projecting images, 564–565, 564f
lateral-line system primordium migration (protocol), 273–275
discussion, 274–275
materials, 273–274
method, 274
motorization, 275
mounting medium, 274
troubleshooting, 274
of live *Phallusia* embryos (protocol), 713–715
long-term imaging of epithelial morphogenesis on three-dimensional organotypic cultures, 623–645
bringing sample to microscope stage (practical), 631–633, 633f
microscope choice, 631–633, 633f
bringing sample to microscope stage (theory), 629–631
differential interference contrast (DIC), 631
end-point analysis of molecular perturbations, 631
end-point phenotype to tissue morphogenetic defect, 631
geometric constraints on sample chamber design, 629–631
media volume, 630
plan for downstream analysis of samples, 630
preferred experimental design with abundant epithelial tissue, 630–631
sample alignment, 629
environmental control, 633–639, 634f
evaporation and gas exchange, 637–638
sample chambers, 638–639, 639f
temperature, 633–637
isolation of mouse mammary organoids for long-term time-lapse imaging (protocol), 640–643
differential centrifugation, 641
experimental method, 640–642
mammary epithelium isolation, 641
mammary gland collection, 640–641
materials, 640
organoid density determination and plating of organoids in Matrigel, 641–642
limiting phototoxicity and photobleaching, 628–629
microscopic requirement issues, 626–628
access to instrument, 627–628
depth of preparation, 626
hardware and software robustness, 627
large number of cells, 626
long movies, 626, 627f
prolonged culture on microscope stage, 628
working distance, 626
overview, 623–625
temperature issues, 633–637
commercial versus homebuilt enclosure systems, 637
heated microscope enclosures, 636
objective lens heater, 635–636
optical drift and, 634
room temperature, 634–635

sample chamber heater, 635
stage-top incubators, 637
mouse kidney cultures, 612
neural crest migration in chick embryo, 90, 91
neuronal development in *Xenopus,* 387–404
image analysis and morphometry, 391, 392f
imaging labeled neurons in living tadpole brain, 390–391
labeling neurons, 388–390
electroporation, 389–390, 390f
fluorescent dextrans, 388
genetic labeling by fluorescent protein expression, 389–390
lipophilic vital dyes, 388–389
overview, 387–388
protocols, 393–403
bulk electroporation of RGCs or CNS neurons in live tadpoles, 399–402
dye labeling retinal ganglion cell axons in live tadpoles, 396–398, 398f
labeling individual neurons in the brains of live tadpoles by electroporation of dyes or DNA, 393–395
recipe, 403
NmuMG/Fucci2 cells, 333–336, 335f
phototoxicity issues, 595
postimplantation mouse embryos, 112–113
quail embryos, 593–604
retinal progenitor lineages in developing zebrafish retina, imaging, 253–268
imaging setup, 254–255
acquisition, 254
processing, 255
overview, 253–254, 267
protocols
DNA injection to generate transiently transgenic retinal progenitor cells, 260
embedding embryos, imaging, staining, and image processing of developing zebrafish retina, 261–267
recipes, 267–268
transplantation of transgenic progenitor retinal cells expressing fluorescent markers, 256–259
strategies for collecting long-term sequences with minimal photodamage, 560–562, 561f
of synaptic protein dynamics, 499–512
synaptogenesis imaging in zebrafish, 412–413, 413f
in vivo imaging of axonal and dendritic structures in developing cortex, 513–522
Xenopus embryos, 70f, 71f, 76–81
examples, 70f, 71f
overview, 76
protocols
construction of simple chambers for high-magnification live imaging of *Xenopus* embryos using inverted microscopes, 79, 79f
high-magnification live imaging of *Xenopus* embryos using confocal microscopy, 80–81, 81f
low-magnification live imaging of intact embryos, 77–78
Total internal reflection fluorescence (TIRF) microscopy
of hippocampal cultures, 463
safe operation of microscope, 833
Trachyphyllia geoffroyi, 92, 276
Transcription, in vitro, 276
Transfection. *See also* Electroporation
of hippocampal neurons, 506–507
of rat hippocampal neurons, 469–471
Transgenics
avian, 92
Drosophila, 29–33
bicoid-green fluorescent protein (Bcd-GFP), 525–526, 528–529, 528f, 529f
transgenic lines for live imaging, 840t–841t
mouse
cell-cycle progression, visualizing spatiotemporal dynamics of multicellular, 331–340
genetic labeling of neurons and, 200–202, 206, 208
imaging egg cylinder stage embryos, 300–301
kidney development imaging, 607–610
lines expressing Cre recombinase, 608–609, 610t
lines expressing fluorescent proteins, 607–608, 607t
quail, 593–594, 597
zebrafish, 51, 62, 62t–63t
for imaging retinal development, 253–267, 430, 430t, 431f
for imaging synaptogenesis, 405–414
Transplantation
in mouse embryo
marking cells for imaging morphogenetic behavior and cell fates, 320–322
advantages and disadvantages of, 327
experimental method, 321–322, 322f
materials, 320
troubleshooting, 322
in zebrafish
of transgenic progenitor retinal cells expressing fluorescent markers, 256–259
dechorionation of embryos, 257–258
experimental method, 257–259
materials, 256–257
Transposase, 32
Transposon-mediated stable integration, 92
Tricaine, 273
Tricaine stock (20×) (recipe), 64–65, 433
Trigeminal sensory neurons
Brainbow imaging of, 196f, 197
in vivo birthdating in zebrafish, 245–250
Trolox (recipe), 489
Ttr promoter, 103, 104
TTR-RFP transgenic line, 300
Tungsten particles, coating
with carbocyanine dyes, 178–180, 179f
with dextran-conjugated fluorescent dyes, 181–182
Two-photon imaging
bicoid morphogen gradient quantification, 524–525, 525f
of dendritic spines, 500–501, 501f
of living chick embryo, 87f
of single-cell electroporation labeled *Xenopus* tectal neurons, 151
Tyrode Ringer's saline, Ca^{2+}/Mg^{++}-free (recipe), 328
Tyrode's solution, 650–651

U

UASp, 32
UAST, 32
Ubiquitin-mediated proteolysis, control of cell cycle by, 332
Ubiquitin promoter, 32
Ubiquitin-proteasome system (UPS), 163
Ultramikroskop, 816
Ultrasound, 77. *See also* Micro-ultrasound imaging
Ultrasound biomicroscopy (UBM), 670, 678
Ureteric bud. *See* Kidney development, imaging

V

Valap (recipe), 243
VAMP, 407f
VAMP/synaptobrevin, 406
Vasculature, dynamic imaging of developing, 660–662, 661f
Vaseline, lanolin, and paraffin (Valap), 243
VDRC, 33
Ventricular septal defects, 647
Vertebrate embryos. See also specific species
optical projection tomography (OPT), 739–752
X-ray microtomographic imaging, 753–764
VGAT, 389, 475
VGluT, 406, 475
Vibratome, 292, 346, 348, 733–734
Viral labeling of chick embryos, 91
Virtual embryo, 706, 707f
Virus-mediated gene delivery
Cre-dependent adeno-associated virus preparation and delivery (protocol), 209–213
genetic labeling of neurons in mouse brain, 205–206, 209–213
Vital dyes
labeling of chick embryos, 91
labeling *Xenopus* neurons for in vivo imaging, 388–389, 393–398
use in zebrafish, 52, 57
Vogt, W., 581
Volocity, 255, 266

W

Water-immersion lens, 561, 632
Watershed ImageJ plugin, 718, 720
Wavelength, 827
Wetzel, R., 581
Wg (*Drosophila*), 29
Whole embryos
challenges in imaging, 817
overview of use, 7–8
Whole-mount in situ hybridization (WMISH), 743, 746
Whole organs, new imaging technologies for, 7
Window method, for imaging *Drosophila melanogaster,* 39–40

Wingless, gradient of, 536
Wnt, 743
WPRE (woodchuck posttranslational regulatory element), 204

X

XCOSM, 439
Xenopus
  axon pathfinding, imaging, 373, 375–380, 384
    experimental method, 376–378
      imaging, 378, 379f
      preparing and mounting embryos, 376–378, 376f, 377f
    imaging setup, 375
    materials, 375
    troubleshooting, 376–378
  bulk electroporation of RGCs or CNS neurons in live tadpoles, 399–402
  calcium transients, imaging in spinal neurons, 357–371
    advantages and limitations, 358
    imaging setup, 358
    overview, 357–358
    protocols
      imaging and analysis of *Xenopus* spinal neurons, 361–364
      perturbation of calcium dynamics in *Xenopus* spinal neurons, 365–368
      preparation of *Xenopus* neuronal tissues for imaging, 359–360
      recipes, 369–370
  fixed embryo preparation for confocal imaging, 729–737, 730f
    protocol, 732–736
      bisection of embryos, 734
      bleaching, 733
      clearing, 733
      experimental method, 733–735
      labeling, 733
      materials, 732
      recipes, 736
      sample chamber construction, 734–735, 735f
      Vibratome sectioning, 733–734
      whole-mount confocal optical sectioning of cleared embryos, 735
  live imaging of embryos, 69–84
    applications
      embryo explants in organotypic culture, 82
      examining cellular morphology with membrane-targeted GFP, 82
      examining subcellular localization of GFP-fusion protein, 82
      range of, 71–72
    examples, 70f, 71f
    general materials, 72
    imaging setup, general, 72
    pros and cons, 69, 71
    protocols, 73–81
      construction of simple chambers for high-magnification live imaging of *Xenopus* embryos using inverted microscopes, 79, 79f
      generation of mosaic embryos for imaging and analysis, 75–76, 75f
      high-magnification live imaging of *Xenopus* embryos using confocal microscopy, 80–81, 81f
      labeling embryos with targeted microinjection on mRNA encoding fluorescent proteins, 73, 74f
      low-magnification live imaging of intact embryos, 77–78
    tools used for, 72
  microscopic magnetic resonance imaging (μMRI), 791–792, 791f
  as model system, 729–731
  morphogenesis, molecular mechanisms and cellular mechanics of, 551–567
    overview, 551–552
    protocols
      assembly of chambers for stable long-term imaging of live tissue, 558–559
      imaging processing and analysis, 563–566
      imaging strategies for collecting long-term time-lapse sequences with minimal photodamage, 560–562
      microsurgical approaches to isolate cells and tissues: explant preparation, 555–557
      recipes, 566
      sample preparation for using live reporters, 553–554
  single-cell electroporation (SCE), 143–155, 389, 390f
    efficiency, factors influencing, 144–146
    electroporation of tadpole tectal neurons (protocol), 149–154
    implementation, 146–148
    labeling individual neurons in the brains of live tadpoles by electroporation of dyes or DNA (protocol), 393–395
    overview, 143, 144
    setup, 145f
  time-lapse imaging of neuronal development, 387–404
    image analysis and morphometry, 391, 392f
    imaging labeled neurons in living tadpole brain, 390–391
    labeling neurons, 388–390
      electroporation, 389–390, 390f
      fluorescent dextrans, 388
      genetic labeling by fluorescent protein expression, 389–390
      lipophilic vital dyes, 388–389
    overview, 387–388
    protocols, 393–403
      bulk electroporation of RGCs or CNS neurons in live *Xenopus* tadpoles, 399–402
      dye labeling retinal ganglion cell axons in live *Xenopus* tadpoles, 396–398, 398f
      labeling individual neurons in the brains of live *Xenopus* tadpoles by electroporation of dyes or DNA, 393–395
      recipe, 403
  X-gal staining, 744–745, 744f
  Xradia MicroXCT, 754
  X-ray microtomography (microCT, μCT), 753–764
    as nondestructive imaging, 740
    overview, 753–754
    principles of, 753–754
    protocol, 755–763
      discussion, 762
      experimental method, 756–761
        embedding, 757–759, 757f–759f
        fixation and staining, 756–757
        imaging, 760–761
      imaging setup, 755
      materials, 755–756
      recipes, 763
      troubleshooting, 761
    resolution, 754

Y

Yellow fluorescent protein (YFP)
  axon labeling, 437, 438–439, 438f, 440f, 447
  in Brainbow imaging, 192f, 194–196, 196f
  fluorescent transgene expression in mouse embryos, 103f, 104
  use in zebrafish, 51

Z

Zebrafish
  anesthetizing embryos, 59, 59f, 273, 274
  axon pathfinding, imaging, 381–383, 384
    experimental method, 382
      imaging, 382, 383f
      preparing and mounting of embryos, 382
    imaging setup, 381
    materials, 381
    troubleshooting, 382
  birthdating, 245–252
    overview, 245–247
      BAPTI (birthdating analysis by photoconverted fluorescent protein tracing in vivo), 245–246, 246f
      BAPTISM (birthdating analysis by photoconverted fluorescent protein tracing in vivo combined with subpopulation markers), 246, 247f
      BrdU labeling compared, 246
    protocol, 248–250
      BAPTI procedure, 249–250
      BAPTISM procedure, 250
      example application, 250
      experimental method, 248–250
      imaging setup, 248
      materials, 248
      photoconversion, 249
      recipes, 251
  Brainbow imaging, 191–198
    example application, 197
    overview, 191–192, 192f
    protocol, 193–196
      cre recombinase introduction, 193–194
      materials, 193
      plasmid selection, 194
      recipes, 197
      troubleshooting, 195–196

transgenic construct, 192f
digital scanned laser light-sheet fluorescence microscopy (DSLM), 819f, 820–823
egg collecting, 54
lateral-line system
anatomy of, 271–272
development of, 272
imaging development of, 271–289
labeling defined cells or subsets of cells by Kaede photoconversion (protocol), 276–278
labeling hair cells and afferent neurons in the posterior lateral-line (PLL) system (protocol), 282–284
labeling second-order neurons in the posterior lateral-line (PLL) system (protocol), 285–287
making mosaic primordia by focal electroporation (protocol), 279–281
time-lapse analysis of primordium migration (protocol), 273–275
innervation of, 271–272
live imaging, 49–68
advantages, 50
applications, 50–51
imaging setup, 52
limitations, 50
overview, 49
protocols, 53–61
constructing a microinjection chamber for zebrafish eggs, 56
imaging development, 58–61, 59f, 60f
injecting DNA or RNA constructs encoding fluorescent protein reporters, 53–55, 54f
intravital dyes to ubiquitously label embryos, 57
recipes, 64–65
tools for fluorescently labeling, 51–52
electroporation, 52
fluorescent proteins, 51
intravital dyes, 52
microinjection of DNA, 51
microinjection of RNA, 51
notochord formation in, 569–579
blastomere injection of cleavage-stage embryos and imaging of labeled cells (protocol), 571–578
discussion, 577
experimental method, 572–576
imaging, 575–576
imaging setup, 571
labeling embryos, 572–573
materials, 571–572
mounting, 574–575
recipes, 578
troubleshooting, 576–577
cell labeling techniques, 570
overview, 569–570
pigments, 50
retina, in vivo imaging of, 416–431
discussion, 430, 430t, 431f
examples, 430, 431f
experimental method, 427–428
image acquisition, 428
imaging setup, 426
materials, 426–427, 427f
mounting embryos, 427–428
transgenic lines expressing in retina, 430t
troubleshooting, 428–429
retinal progenitor lineages in developing retina, imaging, 253–268
imaging setup, 254–255
acquisition, 254
processing, 255
overview, 253–254, 267
protocols
DNA injection to generate transiently transgenic retinal progenitor cells, 260
embedding embryos, imaging, staining, and image processing of developing zebrafish retina, 261–267
recipes, 267–268
transplantation of transgenic progenitor retinal cells expressing fluorescent markers, 256–259
synaptogenesis, imaging, 405–415
advantages and limitations, 414
fluorescence imaging of transgenic embryos (protocol), 410–415
discussion, 414
experimental method, 411–413
imaging setup, 410
injection of DNA, 411–411
materials, 410–411
mounting embryos, 412, 413f
recipes, 414–415
time-lapse data collection, 412–413
fluorescent tagging of synaptic proteins, 406–409, 407f, 408f
bacterial artificial chromosomes (BACs), 408–409, 408f
Gal4-UAS system, 407–408
promoters/enhancers, 407–409
overview, 405–409
coexpression of transgenes, 409, 409f
fluorescent tagging of synaptic proteins, 406–409, 407f, 408f
synaptic puncta, identification of, 414
transgenic lines, 51, 62, 62t–63t
transplantation of retinal cells, 256–259, 258f
Z/EG reporter, 204, 327
Zero-calcium HL3 solution (recipe), 839
z-stacks, time lapses of, 273–274

15 Visualizing Cell Contacts and Cell Polarity in *Caenorhabditis elegans* Embryos

Timothy Walston[1] and Jeff Hardin[2]

[1]Department of Biology, Truman State University, Kirksville, Missouri 63501; [2]Department of Zoology, University of Wisconsin-Madison, Madison, Wisconsin 53706

ABSTRACT

The *Caenorhabditis elegans* embryo is particularly amenable to microscopy and embryological studies because of its short developmental time, transparent shell, and nonpigmented cells. Within the embryo, contacts between cells often establish the polarization of neighboring cells. Experiments on cell contacts past the initial stages of cleavage can currently be performed on the embryo in vivo. The following techniques describe the process of making an agar mount for microscopic visualization, capturing 4D data on the microscope, identifying and highlighting cell contacts between blastomeres, and laser killing of blastomeres to inhibit cell contacts.

Introduction, 229
Protocol A: An Agar Mount for Observation of *C. elegans* Embryos, 231
Protocol B: Acquisition of 4D DIC Microscopic Data to Determine Cell Contacts in Embryos, 235
Protocol C: Analysis of 4D DIC Microscopic Data to Determine Cell Contacts in Embryos, 239
Protocol D: Laser Killing of Blastomeres in *C. elegans*, 241
Recipes, 243
References, 243
Movie Legends, 243

INTRODUCTION

Understanding how cells in the embryo establish polarity and cell fate is important for fully understanding the process of development. *Caenorhabditis elegans* is an excellent model system for studying polarity in the embryo because of its invariant lineage and relatively few numbers of cells in the embryo (Sulston et al. 1983).

The proteins involved in polarizing the one-cell *C. elegans* embryo have been extensively studied and are well understood (reviewed in Gonczy and Rose 2005). Many studies have also examined the establishment of polarity of blastomeres later during embryogenesis. Several studies have shown that cell contacts between the P2 and the EMS blastomere permit and direct the polarity of the EMS spindle and establish the fate of the future daughter cells from EMS, the E and MS blastomeres (Walston and Hardin 2006). Through elegant blastomere isolation and recombination experiments, Goldstein showed the roles of both Src and Wnt signaling pathways in establishing polarity within the EMS blastomere (Goldstein et al. 2006). The four-cell *C. elegans* embryo is particularly amenable to both in vivo and in vitro experimentation. However, beyond the four-cell stage, in vitro embryological

experiments, such as those conducted by Goldstein, are increasingly difficult as individual cell identity is difficult or impossible to ascertain. Understanding how these cell contacts can lead to polarity and cell-fate differences is possible through in vivo experiments, such as examining cell–cell contacts and limiting those contacts through either genetic or mechanical manipulation. An example of this technique is the establishment of polarization of the ABar blastomere through contact with the C blastomere (Walston et al. 2004). To study the effects of this contact, several steps were required. Initially, analysis of images was conducted to determine the contact between the cells (Movie 15-1). The effects of this contact were abrogated through *pal-1* RNA interference, which alters the fate of the C blastomere (Movie 15-2). Second, the ABp blastomere was subjected to laser killing, creating steric hindrance between C and ABar (Movie 15-3). Similar techniques can be used to study contacts between blastomeres throughout development.

Here, we describe the techniques used to conduct these experiments including preparing embryos for visualization on an agar mount, collection of 4D data, analysis of 4D data, and ablation techniques for laser killing of individual blastomeres within the embryo. These techniques focus primarily on the use of differential interphase contrast (DIC) microscopy because of its broad availability, common use for *C. elegans* imaging, and wide applicability to microscopic analysis of embryos of other organisms.

However, many of these techniques are also applicable to fluorescent imaging. The broad range of green fluorescent protein (GFP) markers and other labels that can be visualized in living embryos expands the possibilities of analysis of cell contacts and cell polarization.

Protocol A

An Agar Mount for Observation of *C. elegans* Embryos

The agar mount is an easy way to prepare *C. elegans* embryos for microscopy. The mount slightly embeds the embryo in agar to hold it in place. The mount also slightly compresses the embryo to provide consistent orientation of the embryo such that every embryo will be positioned with either its right side or its left side facing the objective. Other techniques can result in random orientations that complicate analysis and make identification of individual blastomeres more challenging.

IMAGING SETUP

For assembling the mount, a standard stereoscope is required for all steps with *C. elegans*. To identify early embryos (one to four cells), a total zoom of 80x or greater is recommended. We use Leica S8 APO microscopes with 10x eyepieces and Leica MZ12.5 microscopes with 16x eyepieces and 1.0x objective lenses.

MATERIALS

See the end of the chapter for recipes for reagents marked with <R>.

Reagents

Agar (5%)
C. elegans hermaphrodite (gravid)
M9 buffer <R>
Valap <R>

Equipment

See Imaging Setup
Calibrated glass pipettes, 50-µL
Coverslips, 18 x 18-mm (#1)
Eyelash brush (eyelash glued to end of round toothpick)
Mouth pipette 15-in aspirator tube assembly
Microscope slides, 25 x 75 x 1-mm
Platinum wire pick

> One inch of 30-gauge platinum or 90% platinum, 10% iridium wire is inserted into a 6-in pasteur pipette and is heated in a flame until the glass melts around the wire. Flat end hobby pliers or a small tack hammer are used to flatten the end of the pick.

Single-depression microslide, 3-mm
Syringes (1 cc) with 27 gauge x ½-in needles

EXPERIMENTAL METHOD

The total time needed for the experienced is 10–15 min and for the novice is 30 min.

1. Use a platinum wire pick to move approximately five gravid *C. elegans* hermaphrodites from a culture dish to a single-depression microslide mostly filled with M9 buffer.

   The number of hermaphrodites needed will depend on the number of embryos required at the appropriate stage.

2. By holding a syringe with a needle in each hand, place the needles on either side of a hermaphrodite, and draw the flat sides of the tips of the needles across each other to cut the worm in half transversely (Fig. 1A,B). The embryos will be released from the halves of the hermaphrodite. Use an eyelash brush to carefully prod the halves to expel any remaining embryos.

   It is important to cut as close to the vulva as possible to release newly fertilized embryos in the uterus. This step can also be conducted by cutting the worm in half with a #15 curved blade scalpel.

3. Sort embryos using the eyelash brush, and brush together into a group of approximately 10 embryos (Fig. 1C).

   Embryos will tend to stick slightly to each other when grouped. If you desire a certain stage of embryogenesis, it is at this point that the embryo stage should be assessed and should be sorted appropriately. Two-cell stage embryos are the easiest developmental stage to collect.

4. Using laboratory label tape, tape two microscope slides parallel and one slide width apart on the laboratory bench. Place a third slide between the two taped slides (Fig. 2A). Using a 6-in pasteur pipette, place three to four drops of molten 5% agar onto the middle slide. Immediately lay the fourth slide perpendicular to the other three slides over the agar, and press it over the taped slides to flatten the agar before it cools (Fig. 2B).

5. Once the agar has set up, use a razor blade to trim excess agar from the edges of the slides.

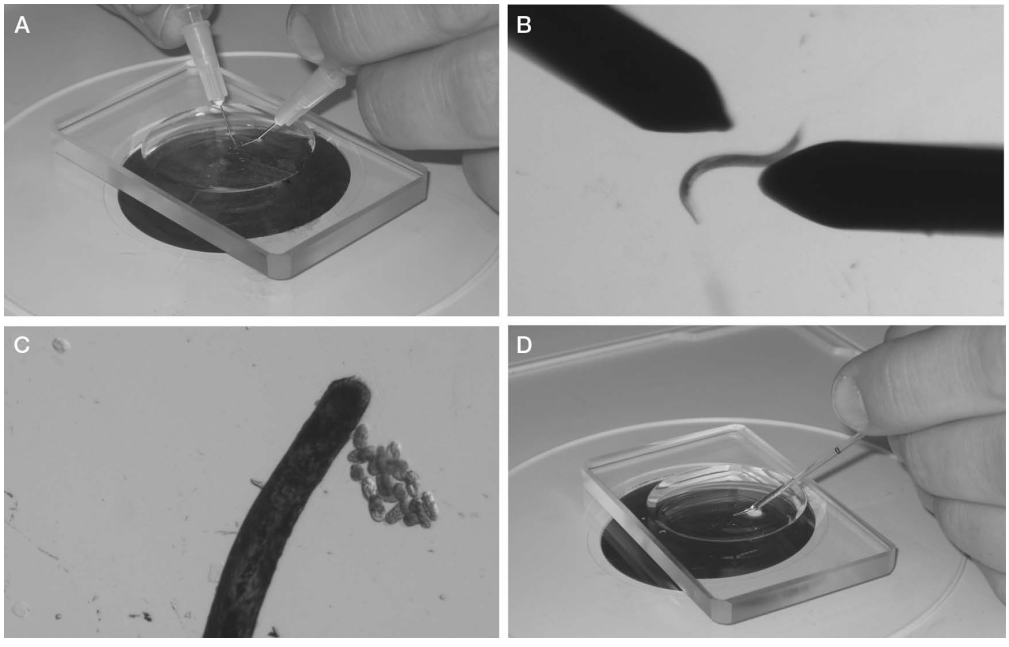

FIGURE 1. Isolation of *C. elegans* embryos and preparation for mounting on a slide. (*A*,*B*) Gravid hermaphrodites are cut in half with 27 x ½-in needles. (*C*) At a higher magnification, embryos are sorted and are grouped using an eyelash. (*D*) Embryos and M9 buffer are transferred using a mouth pipette.

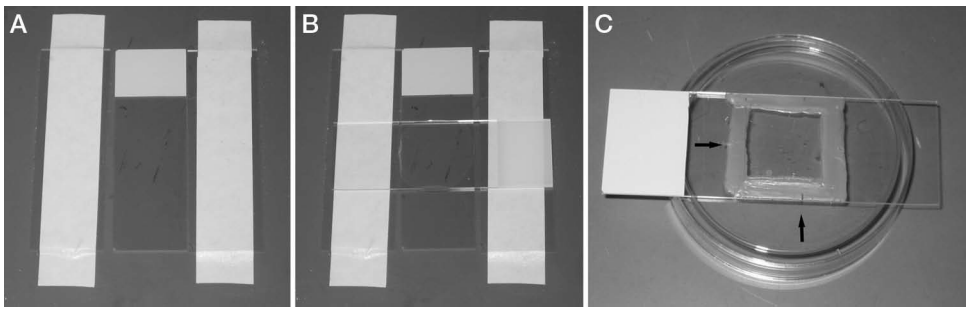

FIGURE 2. Making an agar pad. (*A*) Three slides are placed on the bench, and the outer two are taped down to the bench. (*B*) A drop of molten 5% agar is placed onto the middle slide. A fourth slide is then placed perpendicular to the three original slides. The top slide is compressed over the taped slides. (*C*) The finished slide is sealed with Valap. Using a toothpick to make hash marks in the Valap (arrows) aids in finding the grouping of embryos on the compound scope.

Carefully slide apart the untaped slides so the agar pad is left in the center of one slide.

See *Troubleshooting*.

6. Heat a glass 50-µL pipette in a flame. Once the glass is soft and fluid, remove it from the flame, and quickly pull apart the ends. Break the two ends apart to create a pipette with a tapered end with a diameter of ~40 µm. Place the pipette in a mouth pipette aspirator.
7. Using the mouth pipette, transfer the grouping of embryos (from Step 3) and ~20 µL of M9 to the corner of the agar pad on the microscope slide (Fig. 1D).
8. Brush the embryos out of the M9 into the center of the slide using the eyelash. Position the embryos in a single layer side by side.

   See *Troubleshooting*.
9. Set the edge of a coverslip at the side of the agar pad opposite the M9, and slowly drop it so that the coverslip lands on the embryos before it contacts the M9. Use a Kimwipe to wick excess buffer from the edges of the coverslip, and wick air bubbles from under the coverslip.

   See *Troubleshooting*.
10. Trim excess agar from the edges of the coverslip using a razor blade. Seal the edges of the coverslip with melted Valap using a paintbrush (Fig. 2C).

TROUBLESHOOTING

Problem (Step 5): The agar pad dries to the slide before it can be used.

Solution: Make the pad immediately before use. Stereomicroscopes with light sources mounted under the stage have the potential to heat the stage after long use, which can quickly dry agar pads. Using a stereomicroscope with an external bulb or a cool temperature bulb will reduce this problem.

Problem (Step 8): Embryos fail to develop.

Solution: One-cell embryos are especially vulnerable to mechanical stress and are challenging to mount without killing. If studying a later stage of development, the likelihood of embryos surviving is markedly increased if two-cell or later stage embryos are used to make the mount. Groupings larger than 15–20 embryos often display increased lethality caused by oxygen starvation. By keeping groupings of embryos around 10 embryos, oxygen starvation should not be a problem.

Problem (Step 9): When coverslip is placed on slide, all the embryos wash to the edge of the coverslip.

Solution: Too much M9 buffer is used, and the M9 buffer is hitting the embryos before the coverslip can land on them and hold them in the agar.

Problem (Step 9): The slide has air bubbles under the coverslip.

Solution: Use more M9 buffer. This will allow M9 buffer to completely wash under the coverslip. However, too much M9 buffer will cause embryos to wash away (see previous problem).

DISCUSSION

Mounting *C. elegans* embryos on agar mounts provides a stable long-term environment for microscopic analysis of development. The slight compression from the coverslip will result in embryos reproducibly positioned with either the left or the right side facing toward the objective lens. During later stages of embryogenesis, embryos turn such that left-side views become dorsal views and right-side views become ventral views. Embryos on agar mounts will survive and will hatch from the eggshell on the mount. Embryos prepared with an agar mount are amenable to both light microscopy (with DIC optics) and confocal microscopy.

Alternative methods for mounting embryos, such as poly-L-lysine-coated slides with grease feet (Mohler and Isaacson 2010) or polymer beads (see Chapter 2), are often used to avoid compression to the embryo. However, these techniques typically result in random embryo orientation, which can complicate analysis of development. Additionally, the slight compression of the coverslip seems to have little to no effect on development; and, in most cases, avoidance of such compression is unnecessary.

In conclusion, preparing *C. elegans* embryos on an agar mount is a simple technique that can be easily mastered and is regularly performed by undergraduates in the investigators' laboratories. It provides a consistent embryonic orientation and environment that is suitable for long-term microscopy of *C. elegans* embryos.

Protocol B

Acquisition of 4D DIC Microscopic Data to Determine Cell Contacts in Embryos

Acquisition of stacks of images throughout the thickness of the embryo over time is a crucial method for identifying the positions and contacts between cells. Such 4D microscopy is a routine tool in laboratories that study early *C. elegans* development.

This protocol describes the use of a custom script within μManager's Beanshell scripting language. The script is helpful for reducing the number of shutter open/close events during 4D acquisition. Alternatively, the standard μManager package has been used successfully by one of us (Hardin) to acquire 4D footage, but this involves 20-fold more shutter open/close events than when the script is used. The script is available at http://worms.zoology.wisc.edu/4d/4d.html.

IMAGING SETUP

1. Microscopy/camera hardware: This protocol assumes a basic high-numerical-aperture (high-NA) microscope equipped with oil-immersion objectives and, optionally, an oilable, high-NA condenser from any of the major microscope manufacturers. We typically acquire 4D movies using a 60x–63x, 1.4–1.45-NA PlanApo objective. Older Newvicon video cameras, coupled to the video port on the microscope, are adequate for many applications, especially if they are equipped with a zoomable video lens attachment such as those sold by Nikon. In this case, an AG-5 digitizing board (Scion Corporation) or a similar video frame grabber can be used to digitize the video signal. Alternatively, modern cameras are almost exclusively charge-coupled device (CCD) cameras and have much higher spatial resolution than older video formats. We have successfully used cameras from Scion Corporation and QImaging. The mounting hardware for such devices differs depending on the microscope being used.
2. Cooled environment: We have found that *C. elegans* embryos can be imaged for long periods of time if the ambient temperature is reduced to ~20°C.
3. *z*-axis controller/shutter/serial port: A variety of *z*-axis controllers are available from commercial sources (e.g., Prior Scientific, Ludl Electronics Products, Applied Spectral Imaging [ASI]). In addition, a shutter to block the transmitted light path between time points is strongly encouraged to minimize exposure of embryos to light and to heat.
4. Software: One of us (Walston) has used commercial software (IPLab) to acquire 4D footage. If an inexpensive alternative is desired, free software has been written by one of us (Hardin) as an alternative. Several options are available.
    a. Legacy acquisition plug-ins for ImageJ: These plug-ins are available free of charge at the following URL: http://worms.zoology.wisc.edu/research/4d/4d.html. Full documentation of the plug-ins and detailed instructions for installation of ImageJ and QuickTime for Java are available at the same URL.
    b. μManager: The public domain program μManager supports a variety of CCD cameras, *z* motors, and shutters. The μManager program can be obtained at http://www.micro-manager.org/.

MATERIALS

Reagents

C. elegans embryos, embedded as described in Protocol A
Immersion oil (Type DF oil is recommended)

Equipment

See Imaging Setup.

EXPERIMENTAL METHOD

The total time needed for the experienced is 5 min and for the novice is 15 min.

1. Turn on the *z*-axis and shutter control boxes and the CCD camera. Turn on the light switch on the microscope. Find a group of embryos using the 10× objective, before oiling the coverslip.
2. If a high-NA condenser is present, place a drop of oil on the condenser (for upright microscopes) or on the bottom of the slide (inverted microscopes). Carefully position the condenser so that it contacts the oil and spreads it uniformly between the condenser and the microscope slide.
3. Focus the condenser. The simplest method for achieving good condenser focus is to stop down the condenser using the iris diaphragm, closing it almost completely. Then the height of the condenser can be adjusted at high magnification until the octagonal outline of the diaphragm is in focus. When performed, open the condenser.
4. Once embryos have been located at 10× and the condenser has been focused, swing the 10× objective out of the way, and add a drop of immersion oil to the coverslip (upright microscope) or to the 60× objective lens (inverted microscope). We find that Type DF oil works well.
5. Carefully slide the 60× or the 100× objective into place (it should just clear the sealant on the slide, as long as it is not too thick). Make sure the correct condenser setting is selected to match the lens.
6. Refocus on the embryos, and refocus the condenser.
7. Open μManager. Use the "Live" button in the main μManager Studio window to display an image from the camera. If the "Autoshutter" option is not checked, click the "Open" button to open the shutter. Otherwise, it should open when the "Live" button is clicked. Optimize the positioning of embryos in the field using the stage controls on the microscope and/or by rotating the CCD camera gently by hand (if the mount supports this). Optimize the Nomarski optics through a combination of the following.
   - Center the condenser by closing it and by moving the octagon to the center of the field of view. Reopen the diaphragm to encompass the entire field of view.
   - Adjust the light level. High-quality Nomarski optics requires a substantial amount of light. Optimal settings must be empirically determined.
   - Adjust the exposure time, the gain, and other settings on the CCD camera within.

   Use μManager a final time if needed.

   See *Troubleshooting*.
8. Invoke the μManager 4D acquisition script. This protocol presupposes that a "favorite" has been created previously using the script window in μManager. This window is invoked using the "Tools → Script Panel" menu command in μManager. When the script window appears, select "Acquire_4D.bsh" from the list of favorites. Make sure that the cursor is blinking within the code of this script. Then click "Run". Enter the desired parameters for time interval, number of time points, number of focal planes, and distance between focal planes. Enter the root

name for the images that will be collected. (Note: because most operating systems limit the total length of a file's name to 32 characters, the root name should be kept short.) If a shutter is being used, make sure that the "Use shutter" option is selected.

9. Click "OK." The parameters that have been entered will be displayed. If these are acceptable, click "OK." When prompted for a location to which to save images, make a new directory that will contain the images from the 4D sequence. Within the newly created directory, we recommend making two additional directories: (a) one called "working" and (b) one called "terminal." The latter is useful for acquiring a final *z*-stack of the terminal embryos. Typical settings for a long overnight movie are the following.

   Number of time points: usually 200–300 for an overnight movie
   Time interval (sec): usually 120–180
   Number of shutters: 1
   Number of focal planes: 20
   Distance between focal planes: 1 μm
   Root name: "working," or a short name of choice
   Information for movie: Enter any pertinent information.

   See *Troubleshooting*.

10. Once a directory is specified, the computer should start acquiring images. Status updates will be displayed in the ImageJ main window. To abort, click the "Stop" button in the "Script Panel" window.

11. When the movie is finished, we recommend collecting a terminal image. To do so, keep the field of view the same. Collect a second movie, specifying "1" as the number of time points. Save this movie in the "terminal" folder created previously.

12. To view the movie, there are several options available.

    i. Raw 4D data sets: These can be viewed in one of several ways, including (a) importing the sequences as a "Virtual 5D Stack" within ImageJ, using the "Virtual 5D Stack" plug-in, available on the ImageJ web site, or (b) using the "Browse4D" plug-in available at http://worms.zoology.wisc.edu/4d/4d.html.

    ii. Compressed movies: Movies can also be compressed to save disk space and can be viewed using QuickTime and the "QT4D Writer" and "QT4D Player" plug-ins available at the same URL. If this approach is being used, we typically save the movie using the same root name as the raw files with the word "movie" appended in the same directory created for the experiment. Although many compression algorithms are available, we typically use "Photo/JPEG," "Motion JPEGA," or "Motion JPEGB" compression, "grayscale," and "Medium" quality. This approach can compress movies 30-fold. To play compressed movies, use the QT4D Player plug-in. Select the desired movie. A graphical interface with clickable buttons or the arrow keys on the numeric keyboard can be used to navigate through movies. Once the movie has been successfully compressed and its quality verified, for routine purposes, it is now fine to delete the original files.

TROUBLESHOOTING

Problem (Step 7): No light appears to be reaching the camera.

Solution: Make sure the slider that diverts light from the microscope to the camera port is in the proper position and that the power supply to the camera is on. If the shutter has an external toggle switch, make sure that it is in the correct position. If the exposure time is set to too low a value, increase the exposure time using the controls in the Main μManager window.

Problem (Step 9): The plane of focus drifts systematically over time.

Solution: This often occurs in the first few minutes after making an agar mount. For this reason, it is advisable to check the focus several times during the first 15–20 min of acquisition. To reset the focus, open the shutter, and use the coarse focus on the microscope to refocus on the top focal plane.

Problem (Step 9): Temperature variation in the room results in inconsistent time course of development or variable phenotypes.

Solution: For best results, filming should take place in a room held at constant temperature, ~20°C. Make sure the air conditioner is on and that the door remains closed.

Problem (Step 9): After several hundred time points, μManager reports an error from which it cannot recover.

Solution: Some users have reported errors with μManager when using USB-to-serial port adapters. This is a known issue with μManager. Using a peripheral component interconnect (PCI)–based serial port card appears to alleviate this problem. Alternatively, acquire several shorter movies. We have successfully used this script under μManager for acquiring up to 150 time points with 25 focal planes/time point.

DISCUSSION

This procedure will result in the production of 4D data sets in the form of a series of consecutively named TIFF (tagged image file format) files that can be read by many different programs, including ImageJ, especially when supplemented with appropriate plug-ins. The reduced costs of such a system make this basic system feasible for teaching laboratories and research laboratories constrained by limited funds. Although we have described the use of such a setup for imaging *C. elegans* embryos, this apparatus is well suited for acquiring images of any transparent specimen.

Protocol C

Analysis of 4D DIC Microscopic Data to Determine Cell Contacts in Embryos

Identification of cell contacts is important for understanding how cells within the embryo can be polarized by their neighbors. This protocol will describe a technique for identifying cell contacts and for following those contacts through development. This protocol involves manual segmentation of the membrane of each blastomere from 4D DIC data sets (a wild-type example is shown in Movie 15-1; for comparison, a pal-1(RNAi) embryo is shown in Movie 15-2, and a laser-irradiated embryo is shown in Movie 15-3). Although this technique was performed with *C. elegans* embryos, it will work with any 4D DIC data set. The recent development of a pleckstrin homology (PH)-domain tagged::GFP expressed in *C. elegans* embryos simplifies this analysis (Audhya et al. 2005); however, many organisms lack appropriate GFP transgenes. The use of the GFP transgene advances other fluorescent techniques for labeling the membrane of embryonic cells that required using a laser to carefully permeabilize the eggshell to allow entrance of the dye into the embryo. The technique described below requires only easily obtainable 4D DIC data sets (see Protocol B).

IMAGING SETUP

Previously obtained 4D data sets are required. This technique will specifically address the use of DIC images but can also be extended to confocal images of transgenic embryos.

MATERIALS

Equipment

See Imaging Setup

Computer with image analysis software program and drawing or photograph editing program

A variety of programs can be used for this technique. The image analysis program must have the ability to handle and to easily navigate 4D data sets. The investigators regularly use ImageJ and occasionally use BD Biosciences IPLab. For the drawing or photograph editing program, the investigators have used commercially available Adobe Photoshop and Adobe Photoshop Elements, and freely available versions of ImageJ and GIMP.

Tracing tool

A mouse can be used for this; however, the investigators have had significantly more success using a pen and tablet (such as a Wacom tablet) or the trackpad on a laptop computer.

EXPERIMENTAL METHOD

The total time needed is 15–20 min per time point.

1. Open the 4D data set in the image analysis program. Navigate through time points to the time of interest, and identify the cells of interest. Scroll through the focal planes identifying the focal plane with the closest contact or the clearest contact between the cells.

   See *Troubleshooting*.

   To analyze cell contacts, start the method at least two to three time points before contact or suspected contact.

2. Export all images from that focal plane either to individual frames or to a stack of images.
3. Open the exported images in one of the photograph editing programs. Starting with the first image, select the freehand drawing tool in the software, and use the trackpad or the mouse to trace around the membrane of one of the cells in the embryo.

   The first image analyzed may not be the first time point. In several cases, the investigators found it easier to trace the best contact time point first and to work in either direction in time after that.
4. Selecting a different color, repeat for the other cell being studied for contact. Maintain the color scheme throughout the analysis.
5. Repeat for each time point in the analysis.

   See *Troubleshooting*.

TROUBLESHOOTING

Problem (Step 1): Difficulty determining where the cell membranes are for each cell.

Solution: It is highly recommended to have both the single frame and the 4D data set open at the same time. Membranes that are hard to pick out in the individual frame often are much more obvious in that frame when it can be visualized within the context of the 4D data sets. Often examining neighboring images (either adjacent time steps or adjacent focal steps) can clarify the membrane boundaries in the individual frame. Using a fluorescent membrane marker, such as a PH domain::GFP transgene, highlights membrane boundaries simplifying analysis of cell contacts.

Problem (Step 5): This process takes a lot of time, is there a quicker way to do this?

Solution: Several *C. elegans* laboratories, including the investigators' laboratories, are working on automated or semiautomated segmentation techniques for identifying cell boundaries in images. Until the quality of these techniques can be tested and can be shown to be accurate, hand segmentation of the images is the most accurate way, although it is time consuming. As mentioned above, membrane-based GFP markers also simplify this process and reduce the time for image analysis.

DISCUSSION

This procedure will result in the identification of cell membranes and potential contacts between different blastomeres in the embryo. Although described here for use with *C. elegans* embryos, it could be conducted with any 4D DIC data set. This technique requires particular attention to detail to correctly identify the boundaries of each cell. However, if both a static image and the 4D data set are compared simultaneously, identification of cell boundaries can be completed accurately. Images that use GFPs that label cell boundaries or cell membranes make identification of the boundaries straightforward and require tracing of the boundaries only to highlight and to identify particular cells.

Protocol D

Laser Killing of Blastomeres in *C. elegans*

Blastomere isolation and recombination experiments have led to a wealth of understanding of the events in the four-cell *C. elegans* embryo. However, identifying individual blastomeres after isolation at stages past the four-cell stage is limited. In addition, removal of blastomeres from their native surroundings can interfere with many cell contacts besides the contacts of interest. An alternative approach to studying cell interactions within the *C. elegans* embryo is to use laser ablation of individual cells. Laser ablation can be used to kill one of two cells in contact with each other to understand what happens when a cell no longer signals to its neighbor. Additionally, killing a cell that is between two cells that will eventually contact each other can result in the corpse of the cell forming a steric barrier between the cells preventing the contact. The following protocol describes laser ablation of embryos mounted on an agar mount.

IMAGING SETUP

The laser ablation of *C. elegans* blastomeres requires DIC optics with an ~60x–100x high-NA objective lens. The microscope also requires a tunable dye laser attachment for the lasing and a camera to observe progress of laser killing. A common setup for ablation of *C. elegans* consists of a Micropoint tunable dye laser (Photonic Instruments, Arlington, IL), which includes a 337-nm nitrogen pumping laser and a dye cell filled with Coumarin 440 dye (5 mM in methanol). The intensity of the laser spot can be attenuated using a density gradient filter that slides to generate a spot of the appropriate diameter and intensity as judged by cracking of a coverslip (see below).

MATERIALS

Reagents

C. elegans embryos mounted on an agar mount slide (see Protocol A)

Equipment

See Imaging Setup

EXPERIMENTAL METHOD

The total time needed is 15–30 min.

1. Select embryos on an agar mount.
2. Place embryos on the microscope, and locate them on the slide.
3. Focus the image on the top focal plane of the embryos.
4. Move the focus slightly above the embryos (essentially focusing on the coverslip of the slide), and move the microscope stage to remove embryos from the field of view.
5. Activate a single pulse of the laser. If focused properly, the laser should crack or poke a small hole in the coverslip when pulsed.

   See *Troubleshooting*.

6. Note on the monitor where the pulse cracked the coverslip.

   If using a monitor with a glass screen, marking the spot on the screen with a marker directly on the screen is convenient.

7. Move the microscope stage back to the embryos, and focus on the nucleus of the blastomere to be targeted.

   The target nuclei should be in interphase of the cell cycle and should not be undergoing division.

8. Lase the nucleus of the target cell with ~10 pulses/sec until charcoal buildup can begin to be seen within the nuclei, ~10–15 sec.

   See *Troubleshooting*.

9. Record embryonic development with 4D microscopy.

TROUBLESHOOTING

Problem (Step 5): No hole or crack appears in the coverslip when targeting the laser.
Solution: If no hole appears in the field of view, either the laser is not aimed properly down the objective within the field of view, or the focus is incorrect. The microscope must be focused on the coverslip. If the laser is properly positioned, slightly adjust the focus with the fine-focus control until the coverslip is in focus.

Problem (Step 8): The embryo explodes when laser ablation is attempted.
Solution: If focused too close to the coverslip while targeting the nuclei within a particular embryo, the embryo will rupture as the laser cracks the coverslip. To prevent this, target focal planes of those nuclei deeper within the embryo.

Problem (Step 8): The cell fails to die and continues through development.
Solution: If the target nucleus is not lased sufficiently, it can recover, and the cell will resume mitotic divisions while the embryo progresses through development. Additionally, some cells progress through one final cell division before halting any future divisions. Depending on the particular nature and goals of the experiment, this may or may not be acceptable, and the cell should not be considered killed until cell divisions are halted. Many laser-killed blastomeres will display Brownian motion in which particles in the cytoplasm undergo rapid shaking movements following ablation. This should not be confused with cell division.

Problem: The entire embryo dies rather than an individual blastomere being killed.
Solution: Contrary to the previous problem of not lasing the nucleus long enough, if the entire embryo dies, it is usually caused by excessive lasing triggering embryonic arrest. Practice and experience will provide the best experience with gauging the appropriate amount of lasing to trigger cell death without killing the entire embryo.

DISCUSSION

In cases in which blastomere isolation is not feasible, an alternative is laser killing of particular blastomeres to understand the effects of those blastomeres on development or to create a barrier with the killed cell that prevents other cells from contacting each other. This technique does not require dissecting the embryo, and identification of individual blastomeres at the time of the killing and subsequent to the killing simply requires tracing the lineage of the remaining blastomeres. It can be conducted on embryos throughout development to study cells at a variety of stages of development. This technique can be conducted before 4D imaging or in the middle of collection of a 4D data set without removing the embryo from the microscope if it is set up with both the laser and the 4D imaging equipment.

RECIPES

CAUTION: See Appendix 7 for proper handling of materials marked with <!>.
Recipes for reagents marked with <R> are included in this list.

M9 Buffer

Reagent	Amount
KH_2PO_4	3 g
Na_2HPO_4 <!>	6 g
NaCl	5 g
$MgSO_4$ <!>, 1 M	1 mL
H_2O	to 1 L

Valap

Weigh out a mixture of Vaseline, lanolin, and paraffin (1:1:1[w/w/w]), and place the component in a glass or ceramic vessel. Melt the mixture on a hot plate over medium to low heat until completely liquid. The wax mixture should spread smoothly and should dry quickly on a glass slide. If it hardens too quickly, then add more Vaseline and lanolin. If it does not harden fast enough, then add more paraffin. Valap is solid at room temperature; just before use, warm it at low setting on a hot plate.

REFERENCES

Audhya A, Hyndman F, McLeod IX, Maddox AS, Yates JR 3rd, Desai A, Oegema K. 2005. A complex containing the Sm protein CAR-1 and the RNA helicase CGH-1 is required for embryonic cytokinesis in *Caenorhabditis elegans*. *J Cell Biol* **171:** 267–279.

Goldstein B, Takeshita H, Mizumoto K, Sawa H. 2006. Wnt signals can function as positional cues in establishing cell polarity. *Dev Cell* **10:** 391–396.

Gonczy P, Rose LS. 2005. Asymmetric cell division and axis formation in the embryo. *WormBook*: 1–20.

Mohler WA, Isaacson AB. 2010. Suspended embryo mount for imaging *Caenorhabditis elegans*. *Cold Spring Harb Protoc* doi: 10:1101/pdb.prot.5388.

Sulston JE, Schierenberg E, White JG, Thomson JN. 1983. The embryonic cell lineage of the nematode *Caenorhabditis elegans*. *Dev Biol* **100:** 64–119.

Walston TD, Hardin J. 2006. Wnt-dependent spindle polarization in the early *C. elegans* embryo. *Semin Cell Dev Biol* **17:** 204–213.

Walston T, Tuskey C, Edgar L, Hawkins N, Ellis G, Bowerman B, Wood W, Hardin J. 2004. Multiple Wnt signaling pathways converge to orient the mitotic spindle in early *C. elegans* embryos. *Dev Cell* **7:** 831–841.

MOVIE LEGENDS

Movies are freely available online at www.cshprotocols.org/imaging.

MOVIE 15.1. Contact between the C blastomere and the ABar blastomere directs the spindle orientation of ABar division in a wild-type *Caenorhabditis elegans* embryo. (*Left*) Contact between the C blastomere (membrane near contact outlined in blue) and the ABar blastomere (membrane near contact outlined in green). Focal depth (18

μm) of greatest contact is shown. (*Right*) Shortly after contact between the C and the ABar blastomeres, the mitotic spindle of the ABar blastomere (right line) is shifted toward the contact resulting in a cell division that is perpendicular to orientation of division of the neighboring ABpr blastomere (left line). Focal depth is 7.5 μm.

MOVIE 15.2. Disruption of the fate of the C blastomere using *pal-1(RNAi)* knockdown results in delayed and minimal contact between the C and the ABar blastomeres before division of ABar causing the ABar spindle to be misaligned. (*Left*) Contact is minimal and is delayed between the C blastomere (membrane near contact outlined in blue) and the ABar blastomere (membrane near contact outlined in green). Focal depth (14 μm) of greatest contact is shown. (*Right*) In lieu of a polarizing signal from the C blastomere, the ABar blastomere (right line) adopts the default spindle orientation and divides parallel with the ABpr blastomere (left line). Focal depth is 7 μm.

MOVIE 15.3. Laser killing of ABp creates a barrier between contact with the C and the ABar blastomeres in *Caenorhabditis elegans* embryos. The ABp blastomere (labeled with a red x) was laser killed at the four-cell stage of embryogenesis, just before the start of the movie. The corpse of ABp prevents contact between the C blastomere (membrane near closest contact outlined in blue) and the ABar blastomere (membrane near closest contact outlined in green). Focal depth (10.5 μm) of closest proximity between the two blastomeres is shown. As a result, the ABar blastomere aligns its spindle in the default orientation (line) and divides parallel with the other AB granddaughter cells (not shown).

20 Imaging Cell Movements in Egg Cylinder Stage Mouse Embryos

Shankar Srinivas

Department of Physiology, Anatomy and Genetics, University of Oxford, Oxford OX1 3QX, United Kingdom

ABSTRACT

Cell movements in the pregastrulation egg cylinder mouse embryo play an important role in patterning. The stereotypic movement of the anterior visceral endoderm converts a proximal–distal axis to an anteroposterior axis by properly positioning the primitive streak. The epiblast at this stage is also characterized by a great deal of cell mixing, about which very little is known. Visualizing such cell movements can help us understand their role in embryonic development. This chapter describes a method to isolate, culture, and image the egg cylinder stage mouse embryo.

Introduction, 299
Protocol: Imaging Cell Movements in Pregastrulation Mouse Embryos, 302
Recipe, 309
Acknowledgments, 309
References, 309

INTRODUCTION

Pregastrulation Egg Cylinder Embryo

Before gastrulation, the mouse egg cylinder consists of three tissues: the epiblast, the extraembryonic ectoderm, and the visceral endoderm, which encloses the first two. Although the epiblast gives rise to the majority of fetal tissues, a subset of visceral endoderm cells—the anterior visceral endoderm (AVE)—is responsible for correctly patterning the epiblast. The AVE arises at the distal tip of the egg cylinder and moves unidirectionally to a more proximal position, up to the boundary between the epiblast and extraembryonic ectoderm. It restricts the formation of the primitive streak to the opposite side of the epiblast, thereby inducing anterior neural characteristics in the underlying adjacent epiblast (for review, see Beddington and Robertson 1999; Srinivas 2006; Arnold and Robertson 2009; Rossant and Tam 2009). This movement fails to take place in mutants like *Cripto* (Ding et al. 1998), *Otx2* (Kimura et al. 2000; Perea-Gomez et al. 2001), and *Nodal*$^{lacZ/\Delta 600}$ (Norris et al. 2002), resulting in an incorrectly positioned primitive streak and abnormal embryo development. The mechanism governing the translocation of AVE cells remains poorly understood, although time-lapse studies indicate that it is the result of active migratory movement (Srinivas et al. 2004).

There is significant cell movement in the epiblast of mouse embryos (Gardner and Cockroft 1998). Labeling studies in chick embryos suggest that the hypoblast (the equivalent of the mouse AVE) guides the movement of cells of the overlying epiblast (Foley et al. 2000). This raises the pos-

sibility that cells in the mouse epiblast, rather than moving at random, might do so in a directed manner. Better visualization of cell movements in the epiblast will help untangle this and other outstanding questions.

Transgenic Mice for Imaging Egg Cylinder Stage Embryos

Cell movement in the surface visceral endoderm can be followed using bright-field illumination alone, but generally it is easier and more informative to follow specific cells that have been labeled fluorescently. Cells at this stage can be labeled using dyes such as DiI (Thomas et al. 1998), but there are an increasing variety of transgenic fluorescent reporter mice that make studies of cell movement at this stage easier because they provide embryos in which specific cell types are labeled by the expression of a fluorescent protein. Hex-GFP (Rodriguez et al. 2001) mice express green fluorescent protein (GFP) specifically in the AVE and have been used in time-lapse imaging experiments (see Supplementary Data in Srinivas et al. 2004). Cerl-GFP (Mesnard et al. 2004), Hex-Venus, and Lefty-DsRed2 (Takaoka et al. 2006) transgenes have also been used to label the AVE. Lines that label the entire visceral endoderm include AFP-GFP (Kwon et al. 2006) and TTR-RFP (Kwon and Hadjantonakis 2009).

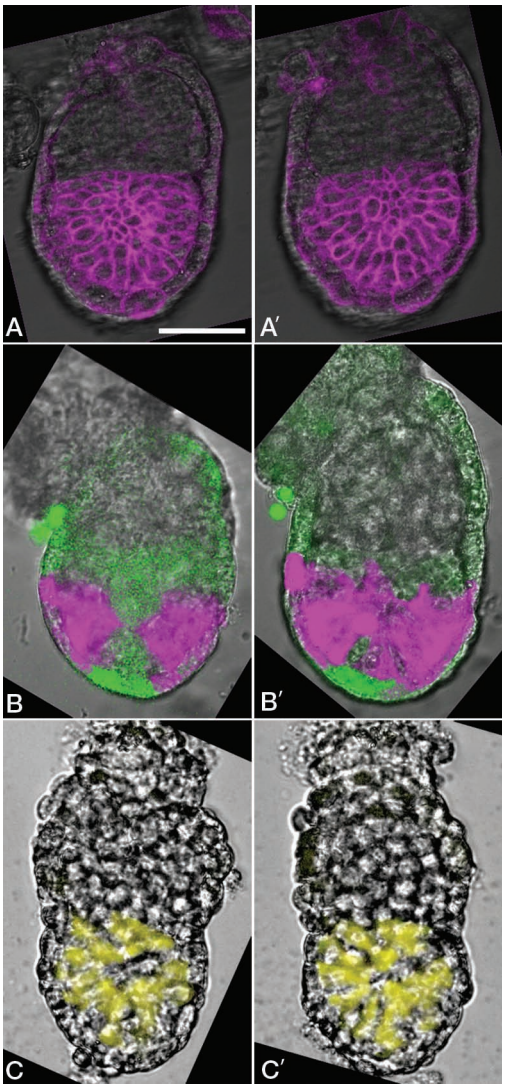

FIGURE 1. Examples of fluorescently labeled mouse embryos. In all three cases, the time between the first and the second image is 2 h. (*A*,*A*′) A CAG-TAG embryo in which the epiblast and visceral endoderm is visualized by expression of a membrane-localized TdTomato (magenta). (*B*,*B*′) A KikGR embryo in which two regions of the epiblast have been labeled by photoconversion (magenta). The green fluorescence is the non-photoconverted KikGR. (*C*,*C*′) An R26R-eYFP reporter embryo in which epiblast cells are labeled (yellow) through the mosaic expression of MORE-Cre. Scale bar, 50 µm.

Mice expressing fluorescent reporters ubiquitously can also be used to visualize cells of the embryo at this stage. Several such lines exist, such as the CAG-TAG line (Trichas et al. 2008), which expresses a membrane-localized TdTomato and nuclear-localized enhanced green fluorescent protein (eGFP) bicistronically. The membrane label allows both movement and changes in cell shape to be followed over time (Fig. 1A). Another strategy useful in following cell movement is to use lines such as CAG-KikGR mice (Kurotaki et al. 2007), which express a photoconvertible protein ubiquitously. Cells can be "labeled" by photoconverting the green KikGR to red using 405-nm light (Fig. 1B). In addition to fluorescent lines, one can also use transgenic Cre driver lines in combination with fluorescent Cre reporters to label specific subsets of cells at this stage. For example, the MORE-Cre line (Tallquist and Soriano 2000) crossed with the R26R-eYFP reporter (Srinivas et al. 2001) labels epiblast cells in a "salt-and-pepper" manner (resulting from the mosaic expression of the Cre), allowing one to follow the movement of individual epiblast cells (Fig. 1C).

The preceding brief discussion of transgenic lines is far from comprehensive and meant only to illustrate some of the approaches possible for labeling cells. Many other useful lines exist, and new lines are being published regularly and can be found though various online resources.

Protocol

Imaging Cell Movements in Pregastrulation Mouse Embryos

Here, we describe how to dissect egg-cylinder stage embryos and an approach for time-lapse imaging of embryos cultured in vivo.

IMAGING SETUP

Microscope

Because the embryo needs to be immersed in medium for culture, an inverted microscope is generally more suitable for imaging. Any compound microscope should be suitable as long as it is equipped with 10×, 20×, and/or 40× objectives and a high-sensitivity camera (such as a cooled CCD camera or a photomultiplier tube on a laser scanning confocal microscope). Ideally, the microscope should also be equipped with automated shutters and control software to take time-lapse images automatically. An automated *x*–*y*–*z* stage is not essential but is a great advantage because it allows several embryos to be imaged over the course of one experiment.

Using just bright-field optics, one can discern cell outlines in the visceral endoderm, but epifluorescence microscopy is essential for more detailed imaging using fluorescently labeled embryos. Standard wide-field epifluorescence, laser scanning, and spinning disk confocal systems are all suitable, and each has its advantages and disadvantages. Confocal microscopes can provide higher-quality images than wide-field epifluorescence microscopes, but they can also be less sensitive and hence lead to more photodamage to the imaged embryo. However, highly sensitive laser scanning confocal microscopes like the Zeiss 710 provide high-quality images with minimal photodamage. High-quality images can also be obtained with specialized wide-field epifluorescence microscopes such as the DeltaVision system (Applied Precision). Objectives such as the Zeiss C-Apochromat 40×/1.2 NA water-immersion lens are particularly suitable because their high numerical aperture allows more light to be collected and because the resulting images they collect suffer fewer aberrations because the refractive index of the immersion medium (e.g., water or a water substitute) is close to that of the culture medium.

Environmental Enclosure

Pregastrulation egg cylinder stage mouse embryos are very sensitive to environmental conditions, particularly temperature fluctuations. Environmental enclosures that maintain the entire microscope at a set temperature are far preferable to stage-top environmental chambers; they generally maintain a more stable temperature and provide more flexibility in terms of the dish used to culture embryos (see Fig. 2A in Chapter 42). Embryos develop better in media that are not buffered with HEPES, and hence the local atmosphere needs to be a humidified 5% CO_2/air mix. This generally can be achieved easily by fashioning a small, clear, plastic box that can be placed on top of the culture dish and into which one can supply premixed 5% CO_2/air that has been bubbled through warm water to humidify it (see Fig. 2B in Chapter 42).

MATERIALS

CAUTION: See Appendix 7 for proper handling of materials marked with <!>.
See the end of the chapter for recipes for reagents marked with <R>.

Reagents

Culture medium
This is a 1:1 mix of heat-inactivated mouse serum (from Step 11) and supplemented CMRL medium. DMEM can be used instead of CMRL, but CMRL gives more consistent results.

Isoflurane <!>
Liquid nitrogen <!>
M2 medium (Sigma-Aldrich)
Mice
Mineral oil, embryo-tested (Sigma-Aldrich)
Supplemented CMRL medium <R>

Equipment

Dissection instruments
Dissection microscope, equipped with transmitted light illumination from below and a fiber optic cold light source for illumination from above
Eppendorf tubes
Fine microdissection forceps
Common forceps are acceptable, provided they have been sharpened on a polishing stone.

Glass-bottomed culture dishes, 35-mm (MatTek) (optional; see note to Step 21)
Lab-Tek II eight-well rectangular chambers, cover glass-bottomed (Nalge Nunc International)
Microscope and analysis software
Needle, 25-gauge
Petri dishes, plastic, 35-mm
Pin vise for holding tungsten needles
P20 Pipetman and pipette tips
Syringe, 1-cc
Tissue culture incubator
Tungsten wire for making needles
For a method for sharpening tungsten needles, see Hogan et al. (1994).

Ultracentrifuge, bench top

EXPERIMENTAL METHOD

Preparation of Mouse Serum

Beddington (1987) presents an alternative approach to preparing rat serum that is also applicable to the preparation of mouse serum.

1. Following a local IACUC-approved procedure, anesthetize the mouse using an inhalant anesthesia (e.g., isoflurane). Kill the mouse by cervical dislocation.
   Be careful to snap the neck cleanly, to avoid internal bleeding from torn blood vessels in the neck.
2. Immediately dissect open the thoracic cavity to expose the heart.
3. Insert a 25-gauge needle (attached to a 1-cc syringe) into the heart; generally, the right ventricle is easiest. Allow the blood to enter the syringe. Facilitate this by gently pulling on the plunger, but do not aspirate the blood by pulling vigorously because this will cause hemolysis.
4. Detach the needle from the syringe. Transfer the blood slowly to an Eppendorf tube.
5. Immediately centrifuge the blood at room temperature at 15,000*g* for 3 min.
   This separates the plasma (top layer) from the cells (bottom layer).

6. Using a sterile pipette tip, collect the plasma. Transfer to a fresh Eppendorf tube on ice.

   Once in the rhythm of things, you should be able to perform Step 6 for the previous sample and Steps 1–4 for the next sample while centrifuging the current sample for 3 min.

7. Incubate all the plasma samples on ice for 3–4 h, during which a fibrin clot will form. At this stage, visually screen the samples and discard those showing extensive hemolysis (i.e., a strong pink color).

8. Centrifuge the samples at 15,000*g* for 10 min at 4°C to pellet the fibrin clot and any residual cells. Collect the serum with a sterile pipette tip.

   If the fibrin clot does not pellet, press it against the wall of the Eppendorf tube with a pipette tip to collapse it, and then aspirate the serum.

9. Pool all the serum collected for the day to minimize variations among individual mice.

10. Aliquot the serum into Eppendorf tubes (500 µL per aliquot is generally suitable). Flash-freeze in liquid nitrogen. Store at –80°C.

11. Prepare heat-inactivated serum.

    i. Puncture the top of an Eppendorf tube containing the mouse serum before inactivation to allow any dissolved inhalant anesthesia to escape.

    ii. Heat-inactivate the serum for 30 min at 55°C.

        Heat-inactivated mouse serum can be used for ~1 wk if stored at 4°C.

Dissection of Pregastrulation Egg Cylinder Stage Embryos

The instructions below are guidelines. Try variations to identify what works best for you.

12. Dissect out the two uterine horns into a dish of room-temperature M2 medium in a 35-mm Petri dish.

    Take care to remove as much attached fat as possible before placing the uterus in the dish; this will keep the medium clearer at later stages, making dissections easier.

13. Starting from any end of the uterus, dissect out the decidua one by one.

    Use a dissection microscope with illumination from above for the following steps.

    i. Grasp the uterus to the left of the deciduum with one pair of forceps. Orient the uterus so that the smooth antimesometrial side is uppermost.

       Make sure that the tip of the forceps extends just beyond the mesometrial extent of the uterus (Fig. 2A) so that when orienting the uterus, it can be stabilized by resting the tip of the forceps on the floor of the plastic dish.

    ii. Using the sharp tip of one arm of another forceps, puncture the antimesometrial uterine wall (Fig. 2B). Slide the forceps arm through the uterus and out the other side (Fig. 2C).

        When poking through the uterus with the forceps, try to span a generous segment of uterine wall, as this opens up a larger "window" and ensures that the subsequent step is very easy.

    iii. Tear the uterine wall by pulling firmly on the forceps, in the direction of the long axis of the uterus.

         This should open the uterine wall, exposing the deciduum (Fig. 2D).

    iv. Very lightly grasp the uterus with half-closed forceps. Slide them along the uterus and beneath the deciduum, freeing it from the uterus (Fig. 2E–H).

    v. Repeat Step 13iv with the next deciduum along the uterus.

       After removing two or three decidua, trim off the uterine tissue from which previous decidua have been removed, so that it does not get in the way.

14. Transfer the decidua to fresh room-temperature M2 in the lid of the 35-mm dish used to isolate the decidua.

    The lid has shorter walls than the actual dish, making the subsequent dissection easier.

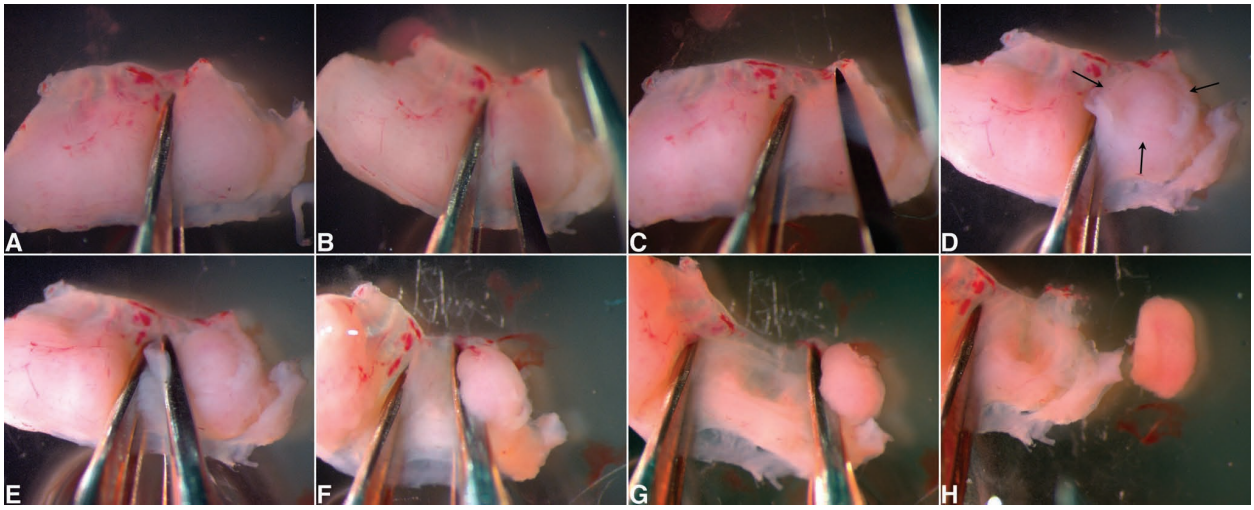

FIGURE 2. Sequence of steps for isolating embryonic day 5.5 (E5.5) deciduum from the uterus. The arrows in *D* show the cut margins of the uterine wall, to indicate how large the opening should ideally be. For details, see Step 13.

15. Dissect out the embryo from each deciduum as follows.

    Switch off the illumination from above, and use only transmitted illumination from below for the following steps.

    i. Orient the deciduum so that the end that has a midline groove (and is slightly blunter) is positioned to the right (Fig. 3A).

    ii. Pin the deciduum down on the dish with a closed set of forceps pressed into the middle of the deciduum, near the inside end of the groove (Fig. 3B).

    iii. Use another set of closed forceps to tear the right half of the deciduum open along the midline in a single motion (Fig. 3B,C).

        Do not make many small cuts, as this will create jagged edges in the deciduum that make it difficult to locate the embryo.

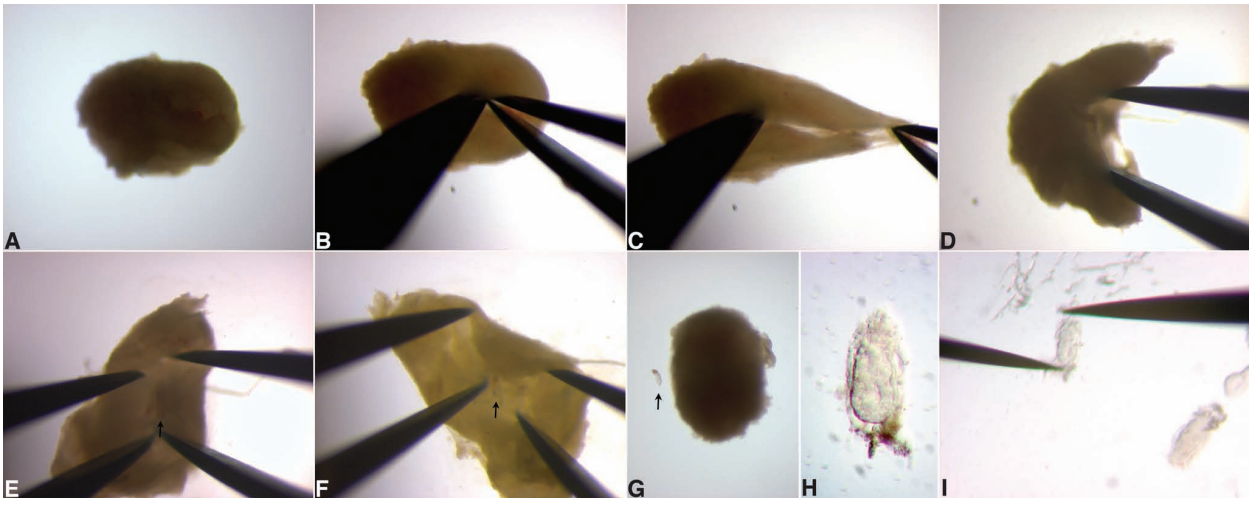

FIGURE 3. (*A–F*) Sequence of steps for isolating an E5.5 embryo from a deciduum. (*G*) An embryo and deciduum next to each other to provide a sense of scale. The embryo in this panel is ~100 µm in width. The arrow in *E–G* points to the embryo. (*H*) An isolated E5.5 embryo, with intact Reichert's membrane. (*I*) Removal of the Reichert's membrane with tungsten needles.

iv. Open up the deciduum by inserting a closed forceps into the tear and allowing the forceps to open. At the same time, pivot the deciduum into a vertical position, with the torn half facing up, so that you can look down into its interior.

v. Pin the open deciduum down on the floor of the dish using forceps. Identify the embryo: It should be visible as a slight shadow, often located near a darkly pigmented structure in the deciduum.

Adjust the angle of the illumination if necessary to see the embryo clearly (Fig. 3D–F).

vi. Pinch into the decidual tissue beneath with forceps. Scoop out the embryo and move it to one side of the dish, so that it is out of the way while isolating embryos from the other decidua.

Embryos can be moved by gently swirling the medium around them with forceps, or by picking them up in a pipette tip. If using a pipette tip, make sure to aspirate M2 medium into the tip once or twice before handling the embryo, as this helps prevent the embryo from sticking to the plastic wall of the tip.

16. After all the embryos have been isolated, remove Reichert's membrane.

Continue using illumination from below on the dissection microscope. Using the following method, with a little practice one can become adept at removing Reichert's membrane quickly and without damage to the embryo. For an alternate approach to removing the membrane using micromanipulators, see Miura and Mishina (2003). For an enzymatic procedure, see Rivera-Perez et al. (2007).

i. Insert one tungsten needle into the space between Reichert's membrane and the embryo to pin down the embryo.

Generally, it is easiest to do this where Reichert's membrane meets the ectoplacental cone. Sometimes, there is also a fair amount of space at the distal tip between the embryo and Reichert's membrane (Fig. 3H,I).

ii. Use a second tungsten needle to peel off Reichert's membrane.

iii. Remove any Reichert's membrane attached to the embryo using the tungsten needles.

When cutting with tungsten needles, hold the needles so that they are opposed and in contact with each other, forming an X shape. To cut, draw the needles apart so that the point of contact between the needles travels toward the tip of the needles (in a manner similar to the action of scissors). This cuts the intervening Reichert's tissues neatly and avoids damaging the embryo.

17. Store embryos in M2 medium for up to 1–2 h, preferably at 37°C.

Imaging Cell Movements in the Egg Cylinder Embryo

18. Equilibrate culture medium for 2–3 h in a tissue culture incubator at 37°C and 5% CO_2.

Medium can also be equilibrated overnight, but preferably for not more than ~18 h.

19. Equilibrate the microscope environmental chamber to 37°C for at least 3–4 h, but preferably overnight.

Temperature stability is important for embryos to culture well, and some components of the microscope (e.g., the objectives) can take several hours to equilibrate.

20. Using a pipette tip, wash away excess M2 medium by transferring the embryos to be imaged into a drop of culture medium.

21. Transfer the embryos into 500 µL of culture medium in one well of an eight-well Lab-Tek II cover glass-bottomed dish.

Alternatively, image embryos in ~300 µL of culture medium in the depression created by the cover glass in MatTek dishes.

22. If imaging for >8–10 h, overlay the medium with embryo-tested mineral oil.

If using MatTek dishes, it is generally best to overlay the medium with mineral oil even for short culture experiments.

23. Position the cover glass-bottomed dish on the microscope stage, ensuring that the local atmosphere is 5% CO_2 in air.

    Make sure the dish has a lid on it; this will minimize both evaporation of medium and also embryo drift during imaging.

24. Select an objective for imaging. Set up the microscope control software to capture images or image volumes at the desired time interval.

    Generally 20× or 40× objectives are suitable for observing the movement of cells in the context of the entire embryo. A time-lapse interval of 8–15 min is a good compromise between good temporal resolution and minimizing photodamage to the embryo. Embryos can be imaged for >12 h under such conditions.

See *Troubleshooting*.

TROUBLESHOOTING

Problem (Step 24): The embryo fails to develop during imaging.
Solution: This could be caused by any number of reasons. Perform controls to determine the cause of the problem.

- Culture embryos in a tissue culture incubator. If the embryos do not develop normally, there likely is a problem with one of the components of the culture medium. Try using freshly prepared medium with new components. Alternatively, small amounts of fixative or other noxious compounds could be compromising the culture. This can happen if, for example, tools used to manipulate embryos in fixative are used to isolate embryos for culture. Try keeping a set of tools exclusively for use with embryos for culture. If possible, isolate embryos in a location as clean as one used for tissue culture.
- Culture embryos in the microscope without imaging. If the embryos do not develop, test the temperature stability within the enclosure. Use a commercially available temperature logger to record the temperature at preset intervals and measure temperature fluctuations over the course of the culture period. Shifts in temperature below 37°C can be as bad for viability as fluctuations above 37°C. A common cause for temperature fluctuations within the microscope enclosure are room air-conditioning vents pointed directly at the microscope.
- Test the pH of the culture medium to confirm that the local CO_2 concentration is correct. If not, adjust the gas flow rate (it generally need not be high for a reasonably air-tight atmospheric enclosure).
- Measure the volume of the culture medium before and after culture to determine if the medium is evaporating. If it is, confirm that the gas is being humidified, or overlay the culture medium with mineral oil.

Problem (Step 24): Embryos do not develop normally when imaged.
Solution: This is indicative of photodamage to the embryo and can be solved by reducing the energy load on the embryo by one or more of the following methods.

- Reduce the frequency of imaging by increasing the time lapse.
- If you are taking image volumes, reduce the number of images in the stack.
- Reduce the exposure time for each image.
- Reduce the illumination intensity.
- If you are using a scanning confocal microscope, reduce the pixel dwell time and/or the scan resolution, so that the total time the embryo is scanned is reduced.

All these approaches will lead to some degree of degradation of data quality. Loss of image brightness can be compensated for to some extent by increasing the gain or by binning. If fluo-

rescence intensity does not need to be quantified and if using a detector that captures at >8-bit depth (i.e., >255 gray levels), one can use a histogram of the distribution of pixel intensities to adjust the exposure time to capture only 8 bits of information per channel, as this is sufficient bit depth for images for figures. Where possible, use fluorophores that are excited at longer, lower energy, wavelengths.

Problem (Step 24): Embryos drift out of the field of view during imaging.

Solution: This can be a difficult problem to avoid. Temperature differences in the vicinity of the sample can set up convection currents in the culture medium. Make sure the environmental enclosure is well equilibrated. The culture dish should be covered with a lid, even if the medium is overlaid with mineral oil. This generally reduces drift, presumably by preventing the incoming CO_2/air mix from causing eddies on the surface of the oil/culture medium that can shift the embryos. If drift is still a problem and there is a risk of losing the embryo from the field of view altogether, try imaging with a lower magnification objective with a larger field of view. A 20× objective is generally a good compromise of magnification and field of view.

RECIPE

Recipes for reagents marked with <R> are included in this list.

Supplemented CMRL Medium

CMRL medium (Invitrogen)	9.9 mL
L-glutamine (100×)	0.1 mL

The supplemented CMRL can be used for ~3 wk if stored at 4°C.

ACKNOWLEDGMENTS

Rosa Beddington gave invaluable guidance in the culture of pregastrulation mouse embryos. I thank Kirstie Lawson for advice on the preparation of serum. I thank the members of my group for their contributions, particularly Vivienne Wilkins for comments on the procedures, Tomoko Watanabe for capturing the photographs of embryo dissections, Georgios Trichas for the image of the CAG-TAG embryo, and Bradley Joyce for the image of the KikGR embryo. Kohei Hatta very kindly shared the KikGR mice with us before publication.

REFERENCES

Arnold SJ, Robertson EJ. 2009. Making a commitment: Cell lineage allocation and axis patterning in the early mouse embryo. *Nat Rev Mol Cell Biol* **10:** 91–103.

Beddington R. 1987. Isolation, culture, and manipulation of post-implantation mouse embryos. In *Mammalian development: A practical approach* (ed. Monk M), pp. 43–69. IRL, Oxford.

Beddington RS, Robertson EJ. 1999. Axis development and early asymmetry in mammals. *Cell* **96:** 195–209.

Ding J, Yang L, Yan Y-T, Chen A, Desai N, Wynshaw-Boris A, Shen MM. 1998. *Cripto* is required for correct orientation of the anterior–posterior axis in the mouse embryo. *Nature* **395:** 702–707.

Foley AC, Skromne I, Stern CD. 2000. Reconciling different models of forebrain induction and patterning: A dual role for the hypoblast. *Development* **127:** 3839–3854.

Gardner RL, Cockroft DL. 1998. Complete dissipation of coherent clonal growth occurs before gastrulation in mouse epiblast. *Development* **125:** 2397–2402.

Hogan B, Beddington R, Costantini F, Lacy E. 1994. *Manipulating the mouse embryo: A laboratory manual*, 2nd ed. Cold Spring Harbor Laboratory Press, Cold Spring Harbor, NY.

Kimura C, Yoshinaga K, Tian E, Suzuki M, Aizawa S, Matsuo I. 2000. Visceral endoderm mediates forebrain development by suppressing posteriorizing signals. *Dev Biol* **225:** 304–321.

Kurotaki Y, Hatta K, Nakao K, Nabeshima Y, Fujimori T. 2007. Blastocyst axis is specified independently of early cell lineage but aligns with the ZP shape. *Science* **316:** 719–723.

Kwon GS, Hadjantonakis A-K. 2009. Transthyretin mouse transgenes direct RFP expression or Cre-mediated recombination throughout the visceral endoderm. *Genesis* **47:** 447–455.

Kwon GS, Fraser ST, Eakin GS, Mangano M, Isern J, Sahr KE, Hadjantonakis A-K, Baron MH. 2006. Tg(Afp-GFP) expression marks primitive and definitive endoderm lineages during mouse development. *Dev Dyn* **235:** 2549–2558.

Mesnard D, Filipe M, Belo JA, Zernicka-Goetz M. 2004. The anterior–posterior axis emerges respecting the morphology of the mouse embryo that changes and aligns with the uterus before gastrulation. *Curr Biol* **14:** 184–196.

Miura S, Mishina Y. 2003. Whole-embryo culture of E5.5 mouse embryos: Development to the gastrulation stage. *Genesis* **37:** 38–43.

Norris DP, Brennan J, Bikoff EK, Robertson EJ. 2002. The Foxh1-dependent autoregulatory enhancer controls the level of Nodal signals in the mouse embryo. *Development* **129:** 3455–3468.

Perea-Gomez A, Lawson KA, Rhinn M, Zakin L, Brûlet P, Mazan S, Ang S-L. 2001. Otx2 is required for visceral endoderm movement and for the restriction of posterior signals in the epiblast of the mouse embryo. *Development* **128:** 753–765.

Rivera-Perez JA, Diefes H, Magnuson T. 2007. A simple enzymatic method for parietal yolk sac removal in early postimplantation mouse embryos. *Dev Dyn* **236:** 489–493.

Rodriguez TA, Casey ES, Harland RM, Smith JC, Beddington RSP. 2001. Distinct enhancer elements control *Hex* expression during gastrulation and early organogenesis. *Dev Biol* **234:** 304–316.

Rossant J, Tam PPL. 2009. Blastocyst lineage formation, early embryonic asymmetries and axis patterning in the mouse. *Development* **136:** 701–713.

Srinivas S. 2006. The anterior visceral endoderm—Turning heads. *Genesis* **44:** 565–572.

Srinivas S, Watanabe T, Lin C-S, William CM, Tanabe Y, Jessell TM, Costantini F. 2001. Cre reporter strains produced by targeted insertion of *EYFP* and *ECFP* into the *ROSA26* locus. *BMC Dev Biol* **1:** 4. doi: 10.1186/1471-213X-1-4.

Srinivas S, Rodriguez T, Clements M, Smith JC, Beddington RSP. 2004. Active cell migration drives the unilateral movements of the anterior visceral endoderm. *Development* **131:** 1157–1164.

Takaoka K, Yamamoto M, Shiratori H, Meno C, Rossant J, Saijoh Y, Hamada H. 2006. The mouse embryo autonomously acquires anterior–posterior polarity at implantation. *Dev Cell* **10:** 451–459.

Tallquist MD, Soriano P. 2000. Epiblast-restricted Cre expression in MORE mice: A tool to distinguish embryonic vs. extra-embryonic gene function. *Genesis* **26:** 113–115.

Thomas PQ, Brown A, Beddington RS. 1998. *Hex*: A homeobox gene revealing peri-implantation asymmetry in the mouse embryo and an early transient marker of endothelial cell precursors. *Development* **125:** 85–94.

Trichas G, Begbie J, Srinivas S. 2008. Use of the viral 2A peptide for bicistronic expression in transgenic mice. *BMC Biol* **6:** 40.